Frequency moments and spectral shape of quantum chains

Alessandro Cuccoli and Valerio Tognetti
Dipartimento di Fisica dell'Università di Firenze, Largo E. Fermi 2, I-50125 Firenze, Italy

Alexei A. Maradudin
Department of Physics, University of California, Irvine, California 92717
and Forum: Project on Condensed Matter Theory of INFM, Firenze-Pisa, Italy

Arthur R. McGurn
Department of Physics, Western Michigan University, Kalamazoo, Michigan 49008
and Forum: Project on Condensed Matter Theory of INFM, Firenze-Pisa, Italy

Ruggero Vaia
Istituto di Elettronica Quantistica del Consiglio Nazionale delle Ricerche, Via Panciatichi 56/30, I-50127 Firenze, Italy
(Received 3 March 1992)

The spectral shape of the displacement correlation function of a quantum chain of atoms interacting through a nearest-neighbor potential is approached at all temperatures and wave vectors by the evaluation of the related frequency moments. The latter ones have been obtained, until the sixth one, by using an effective potential derived by a variational approach to the path-integral formulation of the quantum statistical mechanics. This method allows us to reduce the computation of quantum averages of time-independent functions to classical-like space integrals, so that all the tools developed for classical calculations can be again applied. Explicit results for the Lennard-Jones potential are presented and tested against extensive quantum path-integral Monte Carlo simulations, where an improved Trotter extrapolation procedure is also used. The good agreement between the two calculations confirms the apparent strong simplification introduced by the variational method in the evaluation of the quantum averages when the quantum coupling can be treated semiclassically. The reconstruction of the dynamical behavior of the system through the knowledge of a sufficient number of moments appears realistic. Explicit spectral shapes of Lennard-Jones chains are given, showing the relevance of the quantum effects.

I. INTRODUCTION

In recent years, growing interest has been devoted to the statistical mechanics of physical systems with strong nonlinear interactions, especially low-dimensional systems.[1] This is due to the fact that powerful tools, both analytical and numerical, have become available for their study. From the analytical point of view it has become possible to identify and classify dynamical systems which are completely integrable, i.e., systems for which one can introduce canonical action-angle variables describing both the linear and nonlinear excitations.[2] On the other hand, modern computers permit the exact calculation of the classical thermodynamic quantities of one-dimensional systems, through the transfer-matrix method, and the simulation of the classical thermodynamic behavior of higher-dimensional systems by the use of Monte Carlo algorithms or molecular dynamics. Quantum Monte Carlo techniques have also been developed, but in this case an additional "imaginary-time" dimension must be introduced, and the computing times strongly increase, so that numerical calculations are possible only for quantum systems containing a very small number of particles. The value of methods which allow the reduction of quantum calculations to classical ones, through the introduction of suitable effective potentials, is therefore apparent.

Up to a few years ago, however, this idea could not be usefully applied to solid-state physics. In fact, the best known procedures to obtain effective classical potentials were those introduced by Wigner[3] and Feynman,[4] and both of them possess serious shortcomings when applied to solids. The first one is essentially based on an expansion of the quantum statistical distribution function in powers of $\hbar$ and $\beta=(k_B T)^{-1}$, and therefore becomes rapidly unreliable below the Debye temperature, i.e., in the temperature region where solids reveal their peculiar quantum character. On the other hand, Feynman's original approach defines an effective potential for the free energy by a variational approximation of the path integral starting from the free-particle propagator, which is definitely not a good approximation for the bound particles in a solid.

This situation was radically changed by the recent strong improvement of Feynman's variational method[5–7] obtained by the use of a quadratic trial action. In such a way, the quantum behavior of the harmonic excitations of the system and the classical behavior of the anharmon-

ic part of the potential are fully accounted for in a self-consistent way, so that the thermodynamic properties of solids at high and low temperatures are exactly reproduced and the quantum anharmonic contributions are also taken into account. The method has been applied to the calculation of macroscopic thermodynamic quantities, such as the internal energy and specific heat, of chains with both local and nonlocal nonlinear potentials, with excellent results.[8–10] Very recently the method has been shown to be very useful in the case of rare-gas solids.[11,12]

The effective potential defined in the previous works has a global character and therefore it can be used to evaluate the above-mentioned "global" quantities, but it is not suitable to obtain statistical averages of configuration-dependent functions, i.e., many quantities experimentally accessible. An example is position correlation functions, as probed in neutron-scattering experiments. A correct variational approximation of the (configuration) density, able to take into account the "local" quantum effects of the interaction, must therefore be introduced; this was done for single-particle[13] and two-body[14] interactions. General expressions of the position correlation functions in terms of the effective potential were also derived, and explicit quantum static correlations of the one-dimensional sine-Gordon model have been presented.[15]

Other significant correlation functions, probed by inelastic scattering, are the moments of the dynamic spectral density.[16] They involve functions of momentum and position, so that a generalization of the formalism is required in order to be able to evaluate averages of functions also depending on the momenta. In doing this, particular care has to be taken, due to the noncommutativity of the quantum variables.

The theoretical moments can be directly compared with the experimental data, at least for the first ones. Their knowledge gives important insights about the behavior of the elementary excitations because the knowledge of some number of moments permits the approximate reconstruction of the spectral shape, in terms of a continued fraction expansion[17] and by means of long-time approximations of the dynamic correlation functions.[16,18–20]

In this paper, we present detailed calculations of the moments of the dynamic spectral density of a chain of atoms interacting through a nearest-neighbor Lennard-Jones potential. All the classical moments can be almost entirely calculated analytically by using the extension[21] of a previous approach designed by Gürsey to evaluate the partition function of translation invariant one-dimensional systems.[22] The usefulness of this classical approach, with the introduction of an effective potential in the quantum-mechanical calculation, is apparent.

Monte Carlo (MC) calculations of moments have also been carried out, both in the classical and quantum cases, in order to benchmark the effective potential method and its efficiency in reducing the computational effort. Although MC simulations are restricted to finite chains, we have checked that classical MC for a 30–40-atom chain closely approaches the thermodynamic limit, at least at the higher wave vectors, within numerical uncertainty.

In the last section, we present an approach for the evaluation of dynamical correlations. The dynamical response function, i.e., Fourier transform of the dynamical position correlation function, is calculated using the continued fraction expansion in terms of the moments. Even though the continued fraction can present some problems of convergency, the more significant features due to the quantum character of the atomic vibrations are very well described. We want to point out that this method, improved by the use of the effective potential, is one of the few presently available ones for calculating quantum dynamical correlations of strongly interacting systems.

II. GENERAL FORMALISM FOR QUANTUM THERMODYNAMICS

A. Density matrix and quantum averages

Let us consider a physical system with N degrees of freedom and canonical coordinates $\hat{\mathbf{p}} \equiv \{\hat{p}_1, \ldots, \hat{p}_N\}$ and $\hat{\mathbf{q}} \equiv \{\hat{q}_1, \ldots, \hat{q}_N\}$, $[\hat{q}_i, \hat{p}_j] = i\hbar\delta_{ij}$. Its Hamiltonian is assumed to have the form

$$\hat{\mathcal{H}} = \sum_{i=1}^{N} \frac{\hat{p}_i^2}{2m} + V(\hat{\mathbf{q}}) , \tag{1}$$

and can be thought of as a discretized version of a field-theory model in any dimension and with arbitrary interaction, or as a general model in condensed-matter physics.

Generally, an observable is represented in quantum mechanics by a Hermitian operator (acting on the Hilbert space of the quantum states of the system), which is expressed in terms of the fundamental canonical operators $\hat{\mathbf{p}}$ and $\hat{\mathbf{q}}$. Let $\hat{A} = \hat{A}(\hat{\mathbf{p}}, \hat{\mathbf{q}})$ be an observable. The caret symbol over A [in contrast, e.g., with the notation $V(\hat{\mathbf{q}})$] reminds us that the functional dependence on $(\hat{\mathbf{p}}, \hat{\mathbf{q}})$ is affected by the ordering due to the noncommutativity of the canonical operators.

In the coordinate representation $\hat{q}_i |\mathbf{x}\rangle = x_i |\mathbf{x}\rangle$, the quantum statistical average of $\hat{A} = \hat{A}(\hat{\mathbf{p}}, \hat{\mathbf{q}})$ is given by

$$\langle \hat{A} \rangle \equiv \frac{1}{Z} \mathrm{Tr}(\hat{\rho}\hat{A}) = \frac{1}{Z} \int d\mathbf{x}' d\mathbf{x} \langle \mathbf{x}| \hat{A} |\mathbf{x}'\rangle \rho(\mathbf{x}', \mathbf{x}) , \tag{2}$$

where $\rho(\mathbf{x}', \mathbf{x}) = \langle \mathbf{x}'| e^{-\beta\hat{\mathcal{H}}} |\mathbf{x}\rangle$ is the statistical density matrix at the equilibrium temperature $T = (k_B\beta)^{-1}$ and $\langle \mathbf{x}| \hat{A} |\mathbf{x}'\rangle$ is the matrix representing $\hat{A}$ in the coordinate representation. We shall use the short notation $\rho(\mathbf{x}) \equiv \rho(\mathbf{x}, \mathbf{x})$ for the (configuration) density, in terms of which the partition function Z and the free energy F are defined as

$$Z \equiv e^{-\beta F} \equiv \mathrm{Tr}\hat{\rho} = \int d\mathbf{x} \rho(\mathbf{x}) . \tag{3}$$

If we consider operators $\hat{A} = A(\hat{\mathbf{q}})$, corresponding to observables which depend on the coordinates only, we have $\langle \mathbf{x}| \hat{A} |\mathbf{x}'\rangle = A(\mathbf{x})\delta(\mathbf{x} - \mathbf{x}')$, so that Eq. (2) reduces to

$$\langle A(\hat{\mathbf{q}}) \rangle = \frac{1}{Z} \int d\mathbf{x} \rho(\mathbf{x}) A(\mathbf{x}) . \tag{4}$$

We shall reserve the notation $A(\hat{\mathbf{p}},\hat{\mathbf{q}})$ for the $\hat{\mathbf{p}}$-$\hat{\mathbf{q}}$ ordered form of $\hat{A}$ (i.e., the momentum operators are shifted on the left of their conjugated coordinate operators). In this way we can associate, in a unique way, to any observable $\hat{A}$ a function $A(\mathbf{p},\mathbf{q})$ such that

$$\langle \mathbf{p}|\hat{A}|\mathbf{q}\rangle = \langle \mathbf{p}|\mathbf{q}\rangle A(\mathbf{p},\mathbf{q}) = (2\pi\hbar)^{-N/2} e^{-i\hbar^{-1}\mathbf{p}^T\mathbf{q}} A(\mathbf{p},\mathbf{q}) . \quad (5)$$

For instance, if $\hat{A}=\hat{p}_i\hat{q}_j+\hat{q}_j\hat{p}_i$, then $A(\hat{\mathbf{p}},\hat{\mathbf{q}})=2\hat{p}_i\hat{q}_j+i\hbar\delta_{ij}$ and $A(\mathbf{p},\mathbf{q})=2p_iq_j+i\hbar\delta_{ij}$.

With this in mind, we can express the quantum thermal average (2) of an observable $\hat{A}$ by means of the function $A(\mathbf{p},\mathbf{q})$, since

$$\langle \mathbf{x}|\hat{A}|\mathbf{x}'\rangle = \int d\mathbf{p}\langle \mathbf{x}|\mathbf{p}\rangle\langle \mathbf{p}|\hat{A}|\mathbf{x}'\rangle = \int \frac{d\mathbf{p}}{(2\pi\hbar)^N} e^{i\hbar^{-1}\mathbf{p}^T(\mathbf{x}-\mathbf{x}')} A(\mathbf{p},\mathbf{x}') , \quad (6)$$

and inserting this result in Eq. (2), after a simple replacement of the integration variables, we eventually obtain

$$\langle \hat{A}\rangle = \frac{1}{Z}\int d\mathbf{x}\, A(i\hbar\partial_{\mathbf{z}},\mathbf{x}-\tfrac{1}{2}\mathbf{z})\rho(\mathbf{x}-\tfrac{1}{2}\mathbf{z},\mathbf{x}+\tfrac{1}{2}\mathbf{z})|_{\mathbf{z}=0} , \quad (7)$$

i.e., the momentum $\mathbf{p}$ is replaced by the differential operator $i\hbar\partial_{\mathbf{z}}$, acting on the $\mathbf{z}$ dependence of both A and ρ.

Within Feynman's path-integral formulation of quantum statistical mechanics,[4] the density matrix is expressed by the following integral:

$$\rho(\mathbf{x}',\mathbf{x}) \equiv \langle \mathbf{x}'|e^{-\beta\hat{\mathcal{H}}}|\mathbf{x}\rangle = \int_{\mathbf{x}}^{\mathbf{x}'} \mathcal{D}[\mathbf{q}(u)] e^{-S[\mathbf{q}(u)]} , \quad (8)$$

where the integral is over all paths $\mathbf{q}(u)$, $u\in[0,\beta\hbar]$, having as the initial point $\mathbf{q}(0)=\mathbf{x}$ and as the final point $\mathbf{q}(\beta\hbar)=\mathbf{x}'$. $S[\mathbf{q}(u)]$ is the Euclidean action:

$$S[\mathbf{q}(u)] = \int_0^{\beta\hbar} \frac{du}{\hbar}\left[\frac{m}{2}\dot{\mathbf{q}}^2(u)+V(\mathbf{q}(u))\right] . \quad (9)$$

B. Basic formulas for quantum Monte Carlo

The quantum Monte Carlo (QMC) method is nowadays standard matter, at least in its "plain" version.[23–25] We will derive some formulas here in order to show how averages of $\hat{\mathbf{p}}$-dependent observables can be numerically evaluated. Their basic QMC formulas for the density matrix can be directly derived from Feynman's formula, Eqs. (8) and (9), by discretizing the "imaginary-time" interval $[0,\beta\hbar]$ into an integer number P of equal intervals, so that the variable u takes the discrete values $u_l=\beta\hbar l/P$ ($l=0,1,\ldots,P$), and the path integral is replaced by $P-1$ ordinary (N-dimensional) integrals over the variables $\mathbf{q}_l\equiv\mathbf{q}(u_l)$:

$$\rho(\mathbf{x}',\mathbf{x}) = \left[\frac{mP}{2\pi\hbar^2\beta}\right]^{NP/2}\left[\prod_{l=1}^{P-1}\int d\mathbf{q}_l\right] \times\exp\left\{-\frac{mP}{2\hbar^2\beta}\sum_{l=1}^{P}(\mathbf{q}_l-\mathbf{q}_{l-1})^2 - \frac{\beta}{2P}\sum_{l=1}^{P}[V(\mathbf{q}_l)+V(\mathbf{q}_{l-1})]\right\} , \quad (10)$$

where, according to the prescription of Eq. (8), the paths must begin at $\mathbf{q}(0)=\mathbf{q}_0=\mathbf{x}$ and end at $\mathbf{q}(\beta\hbar)=\mathbf{q}_P=\mathbf{x}'$.

The integer P is usually referred to as the "Trotter number," and, of course, the exact result for $\rho(\mathbf{x},\mathbf{x}')$ is recovered from Eq. (10) in the limit of $P\to\infty$. Actually, when performing numerical calculations, one is restricted to finite P, and the $P=\infty$ results are obtained by extrapolating the numerical outcomes for increasing values of P.

Let us now derive explicit formulas in the case of operators with a simple dependence on $\hat{\mathbf{p}}$, with which we will deal in the following of this paper. From Eq. (4), if $\hat{A}$ is independent of $\hat{\mathbf{p}}$, $\hat{A}=A(\hat{\mathbf{q}})$, we have[23,24]

$$\langle A(\hat{\mathbf{q}})\rangle = \frac{1}{Z}\left[\frac{mP}{2\pi\hbar^2\beta}\right]^{NP/2}\left[\prod_{l=1}^{P}\int d\mathbf{q}_l\right] A(\mathbf{q}_P) \times\exp\left\{-\frac{mP}{2\hbar^2\beta}\sum_{l=1}^{P}(\mathbf{q}_l-\mathbf{q}_{l-1})^2 - \frac{\beta}{P}\sum_{l=1}^{P}V(\mathbf{q}_l)\right\} , \quad (11)$$

and here $\mathbf{q}_0\equiv\mathbf{q}_P$. For a linear dependence on $\hat{\mathbf{p}}$, e.g., $\hat{A}=\hat{p}_jB(\hat{\mathbf{q}})$, we find from Eq. (7), after an integration by parts,

$$\langle \hat{p}_jB(\hat{\mathbf{q}})\rangle = \frac{i\hbar}{Z}\left[\frac{mP}{2\pi\hbar^2\beta}\right]^{NP/2}\left[\prod_{l=1}^{P}\int d\mathbf{q}_l\right] \times\left[\frac{mP}{\hbar^2\beta}(\mathbf{q}_1-\mathbf{q}_P)_j-\frac{\beta}{2P}V_j(\mathbf{q}_P)\right] \times B(\mathbf{q}_P)\exp\left\{-\frac{mP}{2\hbar^2\beta}\sum_{l=1}^{P}(\mathbf{q}_l-\mathbf{q}_{l-1})^2 - \frac{\beta}{P}\sum_{l=1}^{P}V(\mathbf{q}_l)\right\} , \quad (12)$$

where $V_j(\mathbf{x})\equiv\partial V(\mathbf{x})/\partial x_j$. Finally, for an operator which is quadratic in $\hat{\mathbf{p}}$, like $\hat{A}=\hat{p}_i\hat{p}_jB(\hat{\mathbf{q}})$,

$$\langle \hat{p}_i\hat{p}_jB(\hat{\mathbf{q}})\rangle = \frac{-\hbar^2}{Z}\left[\frac{mP}{2\pi\hbar^2\beta}\right]^{NP/2}\left[\prod_{l=1}^{P}\int d\mathbf{q}_l\right] \times\left\{\left[\frac{mP}{\hbar^2\beta}(\mathbf{q}_1-\mathbf{q}_P)_i-\frac{\beta}{2P}V_i(\mathbf{q}_P)\right]\left[\frac{mP}{\hbar^2\beta}(\mathbf{q}_1-\mathbf{q}_P)_j-\frac{\beta}{2P}V_j(\mathbf{q}_P)\right]-\frac{\beta}{2P}V_{ij}(\mathbf{q}_P)-\frac{mP}{\hbar^2\beta}\delta_{ij}\right\} \times B(\mathbf{q}_P)\exp\left\{-\frac{mP}{2\hbar^2\beta}\sum_{l=1}^{P}(\mathbf{q}_l-\mathbf{q}_{l-1})^2-\frac{\beta}{P}\sum_{l=1}^{P}V(\mathbf{q}_l)\right\} , \quad (13)$$

where $V_{ij}(\mathbf{x})=\partial_{x_i}\partial_{x_j}V(\mathbf{x})$.

In order to evaluate the above kinds of averages numerically, the QMC method is implemented by means of the so-called "importance sampling" in configuration space, using, for instance, the well-known Metropolis algorithm.[25] We will apply this method in Sec. VI, where the frequency moments of a nearest-neighbor interacting chain are calculated.

III. VARIATIONAL EVALUATION OF QUANTUM AVERAGES

A. The effective potential and the density matrix

Let us briefly recall the variational method which leads to the definition of a classical effective potential for quantum thermodynamics, introduced by Giachetti and one of us,[5,6] and, independently, by Feynman and Kleinert.[7] It is well known that the analytical evaluation of the path integral (8) is possible only for very simple interaction potentials V, among them those representing a set of free particles (V constant) or a set of harmonic oscillators (V quadratic). Usually the latter model is assumed as starting point for perturbative calculations.[26,27] Long ago Feynman[4] used the free-particle model as the starting point for a variational method in order to evaluate the partition function (3) approximately. He introduced a "trial" action $S_0[\mathbf{q}(u)]$ containing a parameter-function which has to be determined by minimizing with respect to it the rhs of the so-called Feynman-Jensen inequality:[28]

$$F\le F_0+\frac{1}{\beta}\langle S-S_0\rangle_{S_0}\ , \tag{14}$$

where F is the "true" free energy of the system, F_0 the free energy associated with the trial action S_0, and $\langle\cdot\rangle_{S_0}$ the functional average calculated with the path probability distribution e^{-S_0}. However, Feynman's trial action is free-particlelike, so that it cannot account for the quantum harmonic interactions, and it turns out to be useful only above the Debye temperature, where the system behaves almost classically, reproducing the results of the Wigner expansion up to order $\beta^2\hbar^4$.[29]

In order to extend the results to very low temperatures, it is necessary to treat the harmonic part of the field in a fully quantum way. With this aim, Feynman's method was improved[5-7] by making the trial action quadratic, and adding a proper number of variational parameters:

$$S_0[\mathbf{q}(u)]=\int_0^{\beta\hbar}\frac{du}{\hbar}\left[\sum_i\frac{m}{2}\dot{q}_i^2(u)+w(\bar{\mathbf{q}})+\frac{m}{2}[\mathbf{q}(u)-\bar{\mathbf{q}}]^T\cdot\omega^2(\bar{\mathbf{q}})\cdot[\mathbf{q}(u)-\bar{\mathbf{q}}]\right]\ , \tag{15}$$

where

$$\bar{\mathbf{q}}=\bar{\mathbf{q}}[\mathbf{q}(u)]=\frac{1}{\beta\hbar}\int_0^{\beta\hbar}du\ \mathbf{q}(u) \tag{16}$$

is the "average point" of the path. The functional character of $\bar{\mathbf{q}}$ makes the trial action nonlocal, i.e., it does not correspond to any trial Hamiltonian: this point is very important, since it means that we are looking for the best candidate to approximate $S[\mathbf{q}(u)]$ within a very large class of functionals, whose path integrals can still be analytically evaluated, except for the integral over $\bar{\mathbf{q}}$, which is left over as a configuration integral. In addition, this choice of the trial action permits one to reproduce exactly the action corresponding to any quadratic Hamiltonian. Then it is expected that systems like quantum solids, whose low-temperature state can be modeled in terms of quantum linear excitations, can be well described within this framework at any temperature. The parameter functions of S_0 are the c number $w(\bar{\mathbf{q}})$, which was also considered by Feynman, and the $N\times N$ symmetric matrix $\omega^2(\bar{\mathbf{q}})=\{\omega_{ij}^2(\bar{\mathbf{q}})\}$, whose components are the extra parameters of the improved variational method. They are all to be determined by minimizing the right-hand side of the Feynman-Jensen inequality (14). The minimization with respect to $w(\mathbf{x})$ gives[5,6]

$$w(\mathbf{x})=\int V(\mathbf{x}+\xi)\prod_k\frac{d\xi_k}{[2\pi\alpha_k(\mathbf{x})]^{1/2}}e^{-\xi_k^2/2\alpha_k(\mathbf{x})}-\frac{m}{2}\sum_k\omega_k^2(\mathbf{x})\alpha_k(\mathbf{x})\ , \tag{17}$$

where $\xi=\{\xi_i\}$, $\xi_k=\sum_i U_{ki}(\mathbf{x})\xi_i$, $\omega_k^2(\mathbf{x})$ are the N eigenvalues of the matrix $\omega^2(\mathbf{x})$, which is diagonalized by the orthogonal matrix $U(\mathbf{x})$:

$$\omega_k^2(\mathbf{x})\delta_{kl}=\sum_{ij}U_{ki}(\mathbf{x})\omega_{ij}^2(\mathbf{x})U_{lj}(\mathbf{x})\ , \tag{18}$$

and each $\alpha_k(\mathbf{x})$ is a function of $\omega_k(\mathbf{x})$:

$$\alpha_k(\mathbf{x})\equiv\alpha[\omega_k(\mathbf{x})]=\frac{\hbar}{2m\omega_k(\mathbf{x})}\left[\coth f_k(\mathbf{x})-\frac{1}{f_k(\mathbf{x})}\right]\ , \tag{19}$$

$$f_k(\mathbf{x})=\tfrac{1}{2}\beta\hbar\omega_k(\mathbf{x})\ . \tag{20}$$

Note that the parameters α_k can be interpreted as the pure quantum fluctuation (i.e., the difference between the quantum and the classical fluctuation) of the "kth normal mode" with frequency $\omega_k(\mathbf{x})$. The determination (17) also gives $\langle S-S_0\rangle_{S_0}=0$, so that the approximation for F is F_0 itself, and eventually this allows us to define the "global" effective potential

$$V_G(\mathbf{x})=w(\mathbf{x})+\frac{1}{\beta}\sum_k\ln\frac{\sinh f_k(\mathbf{x})}{f_k(\mathbf{x})}\ , \tag{21}$$

which was already obtained in previous works.[5,6] By means of V_G, the quantum free energy is expressed in classical-like form

$$e^{-\beta F}\simeq e^{-\beta F_0}=\left[\frac{m}{2\pi\hbar^2\beta}\right]^{N/2}\int d\mathbf{x}\,e^{-\beta V_G(\mathbf{x})}\ . \tag{22}$$

The variational framework is accomplished after the minimization of F_0 with respect to $\omega^2(\mathbf{x})$:

$$m\omega_{ij}^2(\mathbf{x})=\int \frac{\partial^2 V}{\partial x_i \partial x_j}(\mathbf{x}+\boldsymbol{\xi})\prod_k \frac{d\xi_k}{[2\pi\alpha_k(\mathbf{x})]^{1/2}} e^{-\xi_k^2/2\alpha_k(\mathbf{x})} . \tag{23}$$

At this point, the trial action (15) is fully determined, and we will use it as the best approximation for the true action (9). Replacing $S[\mathbf{q}(u)]$ with $S_0[\mathbf{q}(u)]$, the path-integral definition (8) of the density matrix can be analytically evaluated, and the result can be expressed in terms of the effective potential as

$$\rho(\mathbf{X}-\tfrac{1}{2}\mathbf{z},\mathbf{X}+\tfrac{1}{2}\mathbf{z})=\left[\frac{m}{2\pi\hbar^2\beta}\right]^{N/2}\int d\mathbf{x}\, e^{-\beta V_G(\mathbf{x})}\prod_k \exp\left[\frac{\lambda_k(\mathbf{x})}{2\hbar^2}z_k^2\right]\prod_k \frac{1}{[2\pi\alpha_k(\mathbf{x})]^{1/2}}\exp\left[-\frac{1}{2\alpha_k(\mathbf{x})}(X_k-x_k)^2\right] . \tag{24}$$

The variables with subscript k are obtained, of course, by transformation through $U(\mathbf{x})$, e.g., $x_k=\sum_i U_{ki}(\mathbf{x})x_i$. The parameter

$$\lambda_k(\mathbf{x})\equiv\tfrac{1}{2}m\hbar\omega_k(\mathbf{x})\coth f_k(\mathbf{x})=\gamma_k(\mathbf{x})+\frac{m}{\beta} \tag{25}$$

rules the off-diagonal behavior of $\rho(\mathbf{x}',\mathbf{x})$, and in the last equality the pure quantum part of the momentum fluctuations

$$\gamma_k(\mathbf{x})\equiv m^2\omega_k^2(\mathbf{x})\alpha_k(\mathbf{x}) \tag{26}$$

has been separated from the classical one. It follows that the configuration density reads

$$\rho(\mathbf{X})=\left[\frac{m}{2\pi\hbar^2\beta}\right]^{N/2}\times\int d\mathbf{x}\, e^{-\beta V_G(\mathbf{x})}\times\prod_k \frac{1}{[2\pi\alpha_k(\mathbf{x})]^{1/2}} e^{-(X_k-x_k)^2/2\alpha_k(\mathbf{x})} . \tag{27}$$

The following remarks can be made about the expressions obtained above.

(1) A further Gaussian-like broadening (27) is added with respect to the definition of the effective potential, and the width of the Gaussian depends on the integration variables, so that the evaluation of $\rho(\mathbf{x})$, already difficult when we have only one degree of freedom,[14] becomes very hard for a many-body system: for this reason we will introduce further simplifications in Sec. III C.

(2) As already done for the effective potential (21), the expression for $\rho(\mathbf{x})$ can be compared with the results of the Wigner expansion,[30] and they agree up to terms of order $\hbar^6$ and β^3.[29]

(3) As it is implicit in the choice of the trial action, the results (24) and (27) for the density are exact if the potential V is purely quadratic.

B. Quantum averages

The main result of the variational method described in Sec. III A is Eq. (24). We are now going to use it in order to express quantum average values of physical observables by means of classical-like calculations.

Combining Eqs. (7) and (24), we get the variational approximation for the quantum thermal average of the (p-q-ordered) observable $\hat{A}=A(\hat{\mathbf{p}},\hat{\mathbf{q}})$ as

$$\langle\hat{A}\rangle=\frac{1}{Z}\left[\frac{m}{2\pi\hbar^2\beta}\right]^{N/2}\int d\mathbf{X}\, A(i\hbar\partial_{\mathbf{z}},\mathbf{X}-\tfrac{1}{2}\mathbf{z})\times\int d\mathbf{x}\, e^{-\beta V_G(\mathbf{x})}\prod_k \frac{1}{[2\pi\alpha_k(\mathbf{x})]^{1/2}}\exp\left[-\frac{1}{2\alpha_k(\mathbf{x})}(X_k-x_k)^2-\frac{\lambda_k(\mathbf{x})}{2\hbar^2}z_k^2\right]\Bigg|_{\mathbf{z}=0} . \tag{28}$$

With a further linear variable change we can rewrite this expression as

$$\langle\hat{A}\rangle=\left\langle\left\langle\left[A(i\hbar\partial_{\mathbf{z}},\mathbf{x}+\boldsymbol{\xi}-\tfrac{1}{2}\mathbf{z})\exp\left[-\frac{1}{2}\hbar^{-2}\sum_k\lambda_k(\mathbf{x})z_k^2\right]\right]_{\mathbf{z}=0}\right\rangle_{\mathbf{x}}\right\rangle_G , \tag{29}$$

where we have introduced the shorthand notation $\langle f(\mathbf{x})\rangle_G$ for the classical-like average of a function $f(\mathbf{x})$ with the effective potential $V_G(\mathbf{x})$:

$$\langle f(\mathbf{x})\rangle_G\equiv\frac{1}{Z}\left[\frac{m}{2\pi\hbar^2\beta}\right]^{N/2}\int d\mathbf{x}\, f(\mathbf{x})e^{-\beta V_G(\mathbf{x})} , \tag{30}$$

and the notation $\langle f(\boldsymbol{\xi})\rangle_{\mathbf{x}}$ for the ($\mathbf{x}$-dependent) Gaussian average over the variables $\boldsymbol{\xi}$ defined by

$$\langle f(\boldsymbol{\xi})\rangle_{\mathbf{x}}\equiv\int d\boldsymbol{\xi}\, f(\boldsymbol{\xi})\prod_k\frac{e^{-\xi_k^2/2\alpha_k(\mathbf{x})}}{[2\pi\alpha_k(\mathbf{x})]^{1/2}} . \tag{31}$$

Alternatively, this average can be defined by giving the second moments

$$\langle\xi_i\xi_j\rangle_{\mathbf{x}}=\alpha_{ij}(\mathbf{x})=\sum_k U_{ki}(\mathbf{x})U_{kj}(\mathbf{x})\alpha_k(\mathbf{x}) . \tag{32}$$

With these notations, the effective potential (21) can be written in a more compact way as

$$V_G(\mathbf{x})=\langle V(\mathbf{x}+\boldsymbol{\xi})\rangle_{\mathbf{x}}-\frac{1}{2}\sum_{ij}\alpha_{ij}(\mathbf{x})\left\langle\frac{\partial^2 V}{\partial x_i\partial x_j}(\mathbf{x}+\boldsymbol{\xi})\right\rangle_{\mathbf{x}}+\frac{1}{\beta}\sum_k \ln\frac{\sinh f_k(\mathbf{x})}{f_k(\mathbf{x})} . \tag{33}$$

As in Sec. II B, let us consider the case of some operators with a simple dependence on $\hat{\mathbf{p}}$. The following formulas are easily obtained from Eq. (29):

$$\langle A(\hat{\mathbf{q}})\rangle=\langle\langle A(\mathbf{x}+\boldsymbol{\xi})\rangle_{\mathbf{x}}\rangle_G , \tag{34}$$

$$\langle\hat{p}_j B(\hat{\mathbf{q}})\rangle=\frac{-i\hbar}{2}\left\langle\left\langle\frac{\partial B}{\partial x_j}(\mathbf{x}+\boldsymbol{\xi})\right\rangle_{\mathbf{x}}\right\rangle_G , \tag{35}$$

$$\langle\hat{p}_i\hat{p}_j B(\hat{\mathbf{q}})\rangle=\left\langle\lambda_{ij}(\mathbf{x})\langle B(\mathbf{x}+\boldsymbol{\xi})\rangle_{\mathbf{x}}-\frac{\hbar^2}{4}\left\langle\frac{\partial^2 B}{\partial x_i\partial x_j}(\mathbf{x}+\boldsymbol{\xi})\right\rangle_{\mathbf{x}}\right\rangle_G . \tag{36}$$

Here we have defined the symmetric matrix

$$\lambda_{ij}(\mathbf{x})=\sum_k U_{ki}(\mathbf{x})U_{kj}(\mathbf{x})\lambda_k(\mathbf{x}) . \tag{37}$$

C. The low-coupling approximation (LCA)

For a generic $f(\mathbf{x})$, the average $\langle f(\mathbf{x}+\boldsymbol{\xi})\rangle_{\mathbf{x}}$ can be readily evaluated by expanding $f(\mathbf{x}+\boldsymbol{\xi})$ in power series around the point $\mathbf{x}$, but the remaining average on $\langle\cdots\rangle_G$ is made difficult by the implicit dependence on $\mathbf{x}$ of $\alpha_k(\mathbf{x})$ and $U_{ki}(\mathbf{x})$. Indeed, the self-consistent solutions $\omega_k^2(\mathbf{x})$ and $U_{ki}(\mathbf{x})$ of Eqs. (18) and (23) are to be calculated for any configuration $\mathbf{x}$, and this makes things very complicated, with the exception of the trivial case of a harmonic system, for which Eq. (24) is, by the way, exact. For this reason we introduce a "low-coupling" approximation (LCA), which consists in expanding the renormalization parameters $\alpha_k(\mathbf{x})$ starting from the configuration $\mathbf{x}=\mathbf{x}_0$, for which $V_G(\mathbf{x})$ has its absolute minimum. The idea is that, at low temperatures, due to the weight function $e^{-\beta V_G(\mathbf{x})}$ appearing in Eq. (30), only configurations close to $\mathbf{x}_0$ contribute to the integral. On the other hand, at higher temperatures the parameters $\alpha_k(\mathbf{x})$ rapidly decrease and become less and less dependent on $\mathbf{x}$, and for $T\to\infty$ they reach the Wigner behavior $\alpha_k(\mathbf{x})\simeq\hbar^2\beta/(12m)$. The strong advantage of the LCA is that, for a given temperature, the secular equation (18) has to be solved only once (i.e., for $\mathbf{x}=\mathbf{x}_0$) and that, in the usual case of a translation invariant system, the orthogonal matrix $U(\mathbf{x}_0)$ is a Fourier transformation, as long as the reference configuration $\mathbf{x}_0$ is translation invariant too. If we agree to understand the fixed argument $\mathbf{x}_0$, i.e., $\omega_k\equiv\omega_k(\mathbf{x}_0)$ and so on, the secular equation reads

$$m\omega_k^2\delta_{kl}=\sum_{ij}U_{ki}\frac{\partial^2\tilde{V}}{\partial x_i\partial x_j}(\mathbf{x}_0)U_{lj} . \tag{38}$$

Here, and in the following, the "tilde" denotes the Gaussian smoothing $\tilde{V}(\mathbf{x})\equiv\langle V(\mathbf{x}+\boldsymbol{\xi})\rangle_{\mathbf{x}_0}$. The deviation from the exact eigenvalues can be easily estimated to first order:

$$\delta\omega_k^2(\mathbf{x})\equiv\omega_k^2(\mathbf{x})-\omega_k^2=\sum_{ij}U_{ki}\delta\omega_{ij}^2(\mathbf{x})U_{kj}+O(\epsilon^2) ,$$
$$\delta\omega_{ij}^2(\mathbf{x})\equiv\frac{\partial^2\tilde{V}}{\partial x_i\partial x_j}(\mathbf{x})-\frac{\partial^2\tilde{V}}{\partial x_i\partial x_j}(\mathbf{x}_0) , \tag{39}$$

where we have introduced a label ϵ such that $\delta\omega_k^2(\mathbf{x})=O(\epsilon)$, and ϵ is treated as a small quantity for the reasons discussed above. We can also use a label α for the quantities like α_k, which are small for low quantum coupling at $T=0$ ($\alpha\sim\hbar$) and decrease further for increasing temperature ($\alpha\sim\hbar^2/T$). For instance, after some algebra we find

$$\delta\alpha_{ij}(\mathbf{x})=\sum_{kl}\sum_{i'j'}U_{ki}U_{ki'}\frac{\alpha(\omega_k)-\alpha(\omega_l)}{\omega_k^2-\omega_l^2}\times\delta\omega_{i'j'}^2(\mathbf{x})U_{lj'}U_{lj}+O(\alpha\epsilon^2) , \tag{40}$$

and the analogous expression for $\delta\lambda_{ij}(\mathbf{x})$ has the very same form $[\alpha(\omega)\to\lambda(\omega)]$. In this way, we can approximate the Gaussian averages:

$$\langle f(\mathbf{x}+\boldsymbol{\xi})\rangle_{\mathbf{x}}=\tilde{f}(\mathbf{x})+\frac{1}{2}\sum_{ij}\delta\alpha_{ij}(\mathbf{x})\frac{\partial^2\tilde{f}}{\partial x_i\partial x_j}(\mathbf{x}_0)+O(\alpha\epsilon^2) . \tag{41}$$

When $f(\mathbf{x})$ is translation invariant, this expression becomes much simpler since the Fourier transform of $(\partial^2\tilde{f}/\partial x_i\partial x_j)(\mathbf{x}_0)$ is diagonal,

$$\sum_{ij}U_{ki}U_{lj}(\partial^2\tilde{f}/\partial x_i\partial x_j)(\mathbf{x}_0)\equiv\tilde{f}_k\delta_{kl} ,$$

and we then have

$$\sum_{ij}\delta\alpha_{ij}(\mathbf{x})\frac{\partial^2\tilde{f}}{\partial x_i\partial x_j}(\mathbf{x}_0)=\sum_k\tilde{f}_k\frac{1}{2\omega_k}\frac{\partial\alpha_k}{\partial\omega_k}\delta\omega_k^2(\mathbf{x})+O(\alpha\epsilon^2) . \tag{42}$$

Now, the global effective potential (33) is, in turn, approximated using this equation and expanding the logarithmic term around $\mathbf{x}=\mathbf{x}_0$. Its final expression is

$$V_G(\mathbf{x})=\tilde{V}(\mathbf{x})-\frac{1}{2}\sum_{ij}\alpha_{ij}\tilde{V}_{ij}(\mathbf{x}_0)+\frac{1}{\beta}\sum_k\ln\frac{\sinh f_k}{f_k}+O(\alpha\epsilon^2) . \tag{43}$$

Note that $V_G(\mathbf{x})$ depends on $\mathbf{x}$ through the first term only, so that the derivatives of $V_G(\mathbf{x})$ coincide with the derivatives of $\tilde{V}(\mathbf{x})$.

IV. THE NEAREST-NEIGHBOR INTERACTING CHAIN

In this section we consider the particular case of a one-dimensional lattice of N particles, which can move in the direction of the lattice. They are subjected to a nearest-neighbor (NN) anharmonic interaction $v(x)$,

where x is the NN distance, and to a global constraint of fixed length $L=Na$. In addition, we assume periodic boundary conditions. This rather simple model can be easily generalized to higher-dimensional lattices and more degrees of freedom per particle, i.e., to a model for real anharmonic solids.[12]

The Hamiltonian for this system is Eq. (1), with the potential

$$V(\hat{\mathbf{q}})=\sum_{i=1}^{N} v(\hat{q}_i-\hat{q}_{i-1}) \quad (\hat{q}_0\equiv\hat{q}_N-L) \ . \tag{44}$$

The coordinates $\hat{q}_i$ are defined with respect to some fixed origin, and the spurious coordinate $\hat{q}_0$ again represents the Nth particle, regarded as the backward neighbor of the first one. This model system has already been introduced in Refs. 10 and 31, where the thermodynamic quantities connected to the free energy were calculated. The symbol $\hat{q}$ will be reserved for the position quantum operator, while we will denote the corresponding classical variable with x_i.

A. The frequency moments

In this paper we seek the moments of the spectral density

$$C(k,\omega)=\frac{1}{N}\sum_{ij} e^{-ika(i-j)}\int dt\, e^{i\omega t}\langle[\hat{u}_i(t)-\hat{u}_j(0)]^2\rangle \ . \tag{45}$$

In this expression the wave number k is defined within the first Brillouin zone $[-\pi/a,\pi/a]$, and is quantized in the usual way; $\hat{u}_i(t)\equiv\hat{q}_i(t)-ia$ is the "displacement" of the ith atom at time t. The angular brackets denote the quantum average (2). We have chosen to work with the spectral density (45) because the correlation function which appears as an integrand exists in the thermodynamic limit, while a correlation function of the form of $\langle\hat{u}_i(t)\hat{u}_j(0)\rangle$ does not. The spectral density $C(k,\omega)$ regarded as a function of the frequency ω for a given value of k has peaks centered at the frequencies of the vibrational modes of the chain corresponding to that value of k, whose full width at half maximum is the inverse of the lifetime of these modes.

The function $C(k,\omega)$ defined by Eq. (45) has two important symmetry properties. By expressing the thermal averages in Eq. (45) in terms of the exact eigenfunctions and eigenvalues of the Hamiltonian $\hat{\mathcal{H}}$, it can be shown that $C(k,\omega)=C(-k,-\omega)$. In addition, the fact that every atom in our linear chain is at a center of inversion symmetry has the consequence that $C(k,\omega)=C(-k,\omega)$. Taken together, these properties imply that $C(k,\omega)$ is an even function of both k and ω:

$$C(k,\omega)=C(-k,-\omega)=C(k,-\omega)=C(-k,\omega) \ . \tag{46}$$

We define the frequency moments of $C(k,\omega)$ by

$$\mu_{2n}(k)=\int_{-\infty}^{+\infty} d\omega\,\omega^{2n}C(k,\omega) \ , \tag{47}$$

where we have taken into account the fact that the odd moments vanish in view of Eq. (46). When we combine Eqs. (45) and (47), we find that

$$\mu_{2n}(k)=\frac{2\pi}{N}\sum_{ij} e^{-ika(i-j)} \times\{2\langle\hat{u}^2\rangle\delta_{n0} -(-1)^n[\langle\hat{u}_i^{(2n)}\hat{u}_j\rangle+\langle\hat{u}_j\hat{u}_i^{(2n)}\rangle]\} \ . \tag{48}$$

In this expression $\langle\hat{u}^2\rangle=\langle\hat{u}_i^2\rangle$ is the mean-square displacement of the ith atom. Due to the periodicity of the chain it is independent of the index i. The notation $\hat{u}_i^{(m)}$ stands for

$$\hat{u}_i^{(m)}=\frac{d^m}{dt^m}\hat{u}_i(t)\bigg|_{t=0} \ . \tag{49}$$

The calculation of the moments of $C(k,\omega)$ thus requires the evaluation of equal time correlation functions only.

Before turning to a discussion of how these correlation functions are calculated in the quantum regime and in the classical limit, we note that their calculation can often be simplified by the use of an identity based on the stationarity property

$$\langle\hat{u}_i^{(m)}(t)\hat{u}_j(0)\rangle=\langle\hat{u}_i^{(m)}(0)\hat{u}_j(-t)\rangle \ . \tag{50}$$

We differentiate both sides of this equation n times with respect to t to obtain, on setting $t=0$, the desired result

$$\langle\hat{u}_i^{(m+n)}\hat{u}_j\rangle=(-1)^n\langle\hat{u}_i^{(m)}\hat{u}_j^{(n)}\rangle \ , \tag{51}$$

which is perhaps most useful in the case $m=n$, and tells us that, in order to express the $2n$th moment, it is sufficient to calculate the nth derivative of $\hat{u}_i$:

$$\mu_{2n}(k)=\frac{2\pi}{N}\sum_{ij} e^{-ika(i-j)} \times\{2\langle\hat{u}^2\rangle\delta_{n0} -[\langle\hat{u}_i^{(n)}\hat{u}_j^{(n)}\rangle+\langle\hat{u}_j^{(n)}\hat{u}_i^{(n)}\rangle]\} \ . \tag{52}$$

We now apply the preceding results to the calculation of the moments $\{\mu_{2n}(k)\}$ in the quantum and classical regimes.

1. Quantum regime

In the quantum regime the time derivatives of the displacement $\hat{u}_i$ needed for the calculation of the moments (52) up to the sixth one are obtained by the repeated use of Heisenberg's equation of motion. Thus, we find that

$$\begin{aligned}
\hat{u}_i^{(1)}&=\frac{1}{m}\hat{p}_i \ , \\
\hat{u}_i^{(2)}&=-\frac{1}{m}\frac{\partial\hat{V}}{\partial\hat{u}_i} \ , \\
\hat{u}_i^{(3)}&=-\frac{1}{m^2}\sum_l\left[\hat{p}_l\frac{\partial^2\hat{V}}{\partial\hat{u}_i\partial\hat{u}_l}+\frac{1}{2}i\hbar\frac{\partial^3\hat{V}}{\partial\hat{u}_i\partial\hat{u}_l\partial\hat{u}_l}\right] \ .
\end{aligned} \tag{53}$$

The expression for the moments now become

$$\mu_0(k)=\frac{4\pi}{N}\sum_{ij}\cos[ka(i-j)](\langle\hat{u}^2\rangle-\langle\hat{u}_i\hat{u}_j\rangle)\ ,$$

$$\mu_2(k)=-\frac{4\pi}{N}\sum_{ij}\cos[ka(i-j)]\frac{1}{m}\left\langle\frac{\partial\hat{V}}{\partial\hat{u}_i}\hat{u}_j\right\rangle=-\frac{4\pi}{N}\sum_{ij}\cos[ka(i-j)]\frac{1}{m^2}\langle\hat{p}_i\hat{p}_j\rangle\ ,$$

$$\mu_4(k)=-\frac{4\pi}{N}\sum_{ij}\cos[ka(i-j)]\frac{1}{m^2}\left\langle\frac{\partial\hat{V}}{\partial\hat{u}_i}\frac{\partial\hat{V}}{\partial\hat{u}_j}\right\rangle\ , \tag{54}$$

$$\mu_6(k)=-\frac{4\pi}{N}\sum_{ij}\cos[ka(i-j)]\frac{1}{m^4}\sum_{\ln}\left\{\left\langle\hat{p}_l\hat{p}_n\frac{\partial^2\hat{V}}{\partial\hat{u}_i\partial\hat{u}_l}\frac{\partial^2\hat{V}}{\partial\hat{u}_j\partial\hat{u}_n}\right\rangle\right.$$

$$+i\hbar\left[\left\langle\hat{p}_l\frac{\partial^3\hat{V}}{\partial\hat{u}_i\partial\hat{u}_l\partial\hat{u}_n}\frac{\partial^2\hat{V}}{\partial\hat{u}_j\partial\hat{u}_n}\right\rangle+\left\langle\hat{p}_l\frac{\partial^2\hat{V}}{\partial\hat{u}_i\partial\hat{u}_l}\frac{\partial^3\hat{V}}{\partial\hat{u}_j\partial\hat{u}_n\partial\hat{u}_n}\right\rangle\right]$$

$$\left.-\frac{1}{2}\hbar^2\left[\left\langle\frac{\partial^2\hat{V}}{\partial\hat{u}_i\partial\hat{u}_l}\frac{\partial^4\hat{V}}{\partial\hat{u}_j\partial\hat{u}_l\partial\hat{u}_n\partial\hat{u}_n}\right\rangle+\frac{1}{2}\left\langle\frac{\partial^3\hat{V}}{\partial\hat{u}_i\partial\hat{u}_l\partial\hat{u}_l}\frac{\partial^3\hat{V}}{\partial\hat{u}_j\partial\hat{u}_n\partial\hat{u}_n}\right\rangle\right]\right\}\ .$$

In writing the expression for $\mu_6(k)$, we have kept all the momentum operators to the left of all functions of the displacements, in such a way that Eqs. (11), (12), and (13) or (34), (35), and (36) can be used in order to evaluate the averages by QMC or by the effective potential method presented in Sec. III.

2. Classical regime

In the classical regime the operators $\hat{\mathbf{u}}=\{\hat{u}_i\}$ and $\hat{\mathbf{p}}=\{\hat{p}_i\}$ turn into commuting variables $\mathbf{u}=\{u_i\}$ and $\mathbf{p}=\{p_i\}$, respectively, and a thermodynamic average of the form $\langle f(\mathbf{p})g(\mathbf{u})\rangle$ factors into a Gaussian average over $f(\mathbf{p})$ and the "configuration" average over $g(\mathbf{u})$

$$\langle f(\mathbf{p})g(\mathbf{u})\rangle=\frac{1}{Z}\int d\mathbf{p}\,f(\mathbf{p})e^{-(1/2m)\beta\mathbf{p}^2}\times\int d\mathbf{u}\,g(\mathbf{u})e^{-\beta V(\mathbf{u})}\ , \tag{55}$$

with

$$Z=\int d\mathbf{p}\,e^{-(1/2m)\beta\mathbf{p}^2}\int d\mathbf{u}\,e^{-\beta V(\mathbf{u})}\ . \tag{56}$$

The time derivatives of the displacement u_i needed for the calculation of the moments are obtained from the canonical equations of motion, or, equivalently, from Eqs. (53) by suppressing the "hats" and keeping $\hbar=0$. In the same way, one can directly obtain the classical expressions for the first moments from Eqs. (54), taking into account that the Gaussian averages over the momenta can be decoupled with

$$\langle p_i\rangle=0\ ,\quad\langle p_ip_j\rangle=\frac{m}{\beta}\delta_{ij}\ , \tag{57}$$

so that we eventually get

$$\mu^0(k)=\frac{4\pi}{N}\sum_{ij}\cos[ka(i-j)](\langle u_i^2\rangle-\langle u_iu_j\rangle)\ ,$$

$$\mu_2(k)=-\frac{4\pi}{N}\sum_{ij}\cos[ka(i-j)]\frac{1}{m^2}\langle p_ip_j\rangle=-\frac{4\pi}{m\beta}\ ,$$

$$\mu_4(k)=-\frac{4\pi}{N}\sum_{ij}\cos[ka(i-j)]\frac{1}{m^2}\left\langle\frac{\partial V}{\partial u_i}\frac{\partial V}{\partial u_j}\right\rangle\ , \tag{58}$$

$$\mu_6(k)=-\frac{4\pi}{N}\sum_{ij}\cos[ka(i-j)]\frac{1}{m^3\beta}\sum_l\left\langle\frac{\partial^2V}{\partial u_i\partial u_l}\frac{\partial^2V}{\partial u_j\partial u_l}\right\rangle\ .$$

In the following sections these moments will be evaluated in two different ways: exactly, by an analytic method reported in Ref. 21, where Gürsey's method[22] for the calculation of equilibrium thermodynamic functions of an anharmonic linear chain with nearest-neighbor interactions is extended to the calculation of correlation functions; and by the classical MC simulation method.

B. The effective potential

For the periodic nearest-neighbor chain, the minimum configuration $\mathbf{x}_0$ of the effective potential (21) is, by symmetry, the translation invariant one with $x_{0,i}-x_{0,i-1}=a$. This implies that $U=\{U_{ki}\}$ is a standard (real) Fourier transform,[6] in which the wave number k assumes N values in the first Brillouin zone $[-\pi/a,\pi/a]$. From Eq. (32), the parameters $\alpha_{ij}=\alpha_{ij}(\mathbf{x}_0)$ are simply calculated as

$$\alpha_{ij}=\langle\xi_i\xi_j\rangle_{\mathbf{x}_0}=\frac{1}{N}\sum_k\cos[ka(i-j)]\alpha_k\equiv D_{|i-j|}\ . \tag{59}$$

Their linear combinations

$$\begin{aligned}\mathcal{D}&\equiv\langle(\xi_{i+1}-\xi_i)^2\rangle_{\mathbf{x}_0}\\&=2(D_0-D_1)=\frac{1}{N}\sum_k 4\sin^2\left[\frac{ka}{2}\right]\alpha_k\ ,\\\bar{\mathcal{D}}&=2(D_1-D_2)\\&=\frac{1}{N}\sum_k 4\sin^2\left[\frac{ka}{2}\right]\left[\cos^2\left[\frac{ka}{2}\right]-1\right]\alpha_k\ ,\end{aligned}\tag{60}$$

turn out to be more useful in the following. For instance, we have

$$\tilde{V}(\mathbf{x})=\sum_{i=1}^{N}\tilde{v}(x_i-x_{i-1})\ ,\tag{61}$$

$$\begin{aligned}\tilde{v}(x)&=\langle v(x+\xi_i-\xi_{i-1})\rangle_{\mathbf{x}_0}\\&=\sum_{l=0}^{\infty}\frac{1}{l!}v^{(2l)}(x)\left[\frac{\mathcal{D}}{2}\right]^l\ ,\end{aligned}\tag{62}$$

and the expression for the LCA effective potential Eq. (43) becomes, in this case,[10]

$$V_g(\mathbf{x})=\sum_{i=1}^{N}v_G(x_i-x_{i-1})\ ,\tag{63}$$

$$\begin{aligned}v_G(x)&=\sum_{l=0}^{\infty}\frac{1}{l!}[v^{(2l)}(x)-lv^{(2l)}(a)]\left[\frac{\mathcal{D}}{2}\right]^l\\&\quad+\frac{1}{\beta}\frac{1}{N}\sum_k\ln\frac{\sinh f_k}{f_k}\ .\end{aligned}\tag{64}$$

From Eq. (38) we eventually get the self-consistently renormalized eigenfrequencies

$$\omega_k^2=\frac{\tilde{v}''(a)}{m}4\sin^2\left[\frac{ka}{2}\right]\ .\tag{65}$$

V. ANALYTIC EXPRESSIONS FOR THE MOMENTS

The present section is devoted to the evaluation of moments for the NN interacting chain by means of the method described in Ref. 21. The method will be applied first to the bare potential, in order to obtain the classical results, and next to the LCA effective potential to describe the quantum behavior.

A. Classical regime

To obtain the zeroth classical moment we must consider $\langle(u_{i+p}-u_i)^2\rangle$, which is readily deduced from the equations given in Ref. 21:

$$\langle(u_{i+p}-u_i)^2\rangle=p\left[\frac{\mathcal{F}''(s_0)}{\mathcal{F}(s_0)}-a^2\right]\ ,\tag{66}$$

where

$$\mathcal{F}(s_0)=\int_0^{\infty}dx\,e^{-s_0x}e^{-\beta v(x)}\ ,\tag{67}$$

and the parameter s_0 is determined by the equation of state for the chain

$$\frac{1}{\mathcal{F}(s)}\frac{d\mathcal{F}(s)}{ds}\bigg|_{s=s_0}=-a\ .\tag{68}$$

Finally, by evaluating the sum over i and j appearing in the first of the Eqs. (58), we obtain, for $k\neq 0$,

$$\mu_0^C(k)=-4\pi\left[\frac{\mathcal{F}''(s_0)}{\mathcal{F}(s_0)}-a^2\right]\frac{1}{4\sin^2(ka/2)}\ .\tag{69}$$

The classical second moment is independent of the interaction potential and its evaluation is fully analytical. The final result, already given in Eq. (58), is

$$\mu_2^C(k)=-4\pi\frac{k_BT}{m}\ .\tag{70}$$

In the expression for the fourth moment (58) appear the derivatives of the potential which, for a nearest-neighbors interaction, read

$$\frac{\partial V}{\partial u_i}=v'(x_i-x_{i-1})-v'(x_{i+1}-x_i)\ ,\tag{71}$$

so that we are faced with the evaluation of

$$\left\langle\frac{\partial V}{\partial u_{i+p}}\frac{\partial V}{\partial u_i}\right\rangle=\langle[v'(x_{i+p}-x_{i+p-1})-v'(x_{i+p+1}-x_{i+p})][v'(x_i-x_{i-1})-v'(x_{i+1}-x_i)]\rangle\ .\tag{72}$$

If we introduce the symbols

$$\begin{aligned}\mathcal{W}_n&=\frac{1}{\mathcal{F}(s_0)}\int_0^{\infty}dx\,e^{-s_0x}v^{(n)}(x)e^{-\beta v(x)}\ ,\\\mathcal{W}_{nm}&=\frac{1}{\mathcal{F}(s_0)}\int_0^{\infty}dx\,e^{-s_0x}v^{(n)}(x)v^{(m)}(x)e^{-\beta v(x)}\ ,\end{aligned}\tag{73}$$

where $v^{(n)}$ denotes the nth derivative of v with respect to its argument, we obtain

$$\left\langle\frac{\partial V}{\partial u_{i+p}}\frac{\partial V}{\partial u_i}\right\rangle=(\mathcal{W}_{11}-\mathcal{W}_1^2)(2\delta_{p,0}-\delta_{p,1}-\delta_{p,-1})\ .\tag{74}$$

Now we can observe that, by partial integration

$$\begin{aligned}\mathcal{W}_{11}&=k_BT(\mathcal{W}_2-s_0\mathcal{W}_1)\ ,\\\mathcal{W}_1&=-s_0k_BT\ ,\end{aligned}\tag{75}$$

so that Eq. (74) reduces to

$$\left\langle\frac{\partial V}{\partial u_{i+p}}\frac{\partial V}{\partial u_i}\right\rangle=k_BT\mathcal{W}_2(2\delta_{p,0}-\delta_{|p|,1})\ ,\tag{76}$$

and the evaluation of the spatial Fourier transform finally gives

$$\mu_4^C(k)=-4\pi\frac{k_BT}{m^2}\mathcal{W}_2 4\sin^2\left[\frac{ka}{2}\right]. \quad (77)$$

In a similar way, starting from

$$\frac{\partial^2 V}{\partial u_i \partial u_l}=[v''(x_i-x_{i-1})+v''(x_{i+1}-x_i)]\delta_{i,l} - v''(x_i-x_{i-1})\delta_{i-1,l} - v''(x_{i+1}-x_i)\delta_{i+1,l}\,, \quad (78)$$

we obtain for the average appearing in expression (58) for $\mu_6(k)$:

$$\sum_l\left\langle\frac{\partial^2 V}{\partial u_{i+p}\partial u_l}\frac{\partial^2 V}{\partial u_i\partial u_l}\right\rangle=(4\mathcal{W}_{22}+2\mathcal{W}_2^2)\delta_{p,0} -2(\mathcal{W}_{22}+\mathcal{W}_2^2)\delta_{|p|,1}+\mathcal{W}_2^2\delta_{|p|,2}\,. \quad (79)$$

The classical sixth moment is thus given by

$$\mu_6^C(k)=-4\pi\frac{k_BT}{m^3}\left[16\mathcal{W}_2^2\sin^4\left[\frac{ka}{2}\right] +8(\mathcal{W}_{22}-\mathcal{W}_2^2)\sin^2\left[\frac{ka}{2}\right]\right]. \quad (80)$$

B. Quantum regime

The calculation of moments in the quantum regime can be accomplished, without going into excessively cumbersome expressions, in the LCA approximation. In the following we will obtain explicit results for the first four even moments up to terms of order $\varepsilon\alpha$. Within this approximation, by using Eq. (41) and expanding the terms with "tilde," Eqs. (34) and (36) can be replaced by

$$\langle A(\hat{\mathbf{q}})\rangle=\langle A(\mathbf{x})\rangle_G+\frac{1}{2}\sum_{ij}\alpha_{ij}\left\langle\frac{\partial^2 A}{\partial x_i\partial x_j}(\mathbf{x})\right\rangle_G +\frac{1}{2}\sum_{ij}\langle\delta\alpha_{ij}(\mathbf{x})\rangle_G\frac{\partial^2 A}{\partial x_i\partial x_j}(\mathbf{x}_0)+O(\alpha\varepsilon^2) \quad (81)$$

and

$$\left\langle\sum_{ij}\hat{p}_i\hat{p}_j A_{ij}(\hat{\mathbf{q}})\right\rangle=\sum_{ij}[(mk_BT\delta_{ij}+\gamma_{ij})\langle A_{ij}(\mathbf{x})\rangle_G+\langle\delta\gamma_{ij}(\mathbf{x})\rangle_G A_{ij}(\mathbf{x}_0)] +\frac{1}{2}mk_BT\sum_{ill'}\left[\alpha_{ll'}\left\langle\frac{\partial^2 A_{ii}}{\partial x_l\partial x_{l'}}(\mathbf{x})\right\rangle_G+\langle\delta\alpha_{ll'}(\mathbf{x})\rangle_G\frac{\partial^2 A_{ii}}{\partial x_l\partial x_{l'}}(\mathbf{x}_0)\right]+O(\alpha\varepsilon^2)\,. \quad (82)$$

To obtain the quantum moments we have to evaluate averages of expressions which depend on the configuration through the potential and its derivatives. In the LCA scheme, however, as explained in Sec. III C, we consider that the quantum effects are mainly related to the configuration of minimal potential energy, and this allowed us to expand $\omega^2(\mathbf{x})$ around $\mathbf{x}_0$. In order to be consistent, we have to apply the same approximation everywhere in the quantum terms, so that in all of them we will replace $\partial^n V(\mathbf{x})$ with $\partial^n V(\mathbf{x}_0)+\delta\partial^n V(\mathbf{x})$ and, by considering $\delta\partial^n V(\mathbf{x})$ as $O(\varepsilon)$, we will retain only terms of first order in ε. In some instances, as noted in Ref. 10, the effective potential at the lowest order in α (i.e., the use of the bare frequency) is not sufficient to obtain accurate enough results, and it is important to allow for the self-consistent renormalization of ω_k^2 contained in Eq. (38), even though it implicitly reintroduces higher-order terms in α in the various expressions. In such occurrences, Eqs. (81) and (82) can still be used, if the consistency between the terms containing the renormalized frequencies and those containing the derivatives of the potential is restored by using the substitution $\partial^2 V(\mathbf{x})\simeq\partial^2\tilde{V}(\mathbf{x}_0)+\delta\partial^2 V(\mathbf{x})$ instead of the previous one for $n=2$.

By observing that all the functions $f_{ij}(\mathbf{x}_0)$ appearing in the expressions of the moments are translation invariant, we are allowed to use Eq. (42), so that

$$\sum_{ij}\langle\delta\alpha_{ij}\rangle_G f_{ij}(\mathbf{x}_0)=\sum_k f_k\frac{1}{2\omega_k}\frac{\partial\alpha_k}{\partial\omega_k}\langle\delta\omega_k^2\rangle_G\,, \quad (83)$$

where

$$\langle\delta\omega_k^2(\mathbf{x})\rangle_G=4\sin^2\left[\frac{ka}{2}\right]\frac{\langle v''(x)\rangle_G-v''(a)}{m} =\omega_k^2\left[\frac{\mathcal{W}_{2G}-v''(a)}{\tilde{v}''(a)}\right]. \quad (84)$$

Similar conclusions are valid for terms in $\delta\gamma$, with α replaced by γ.

Finally, the symbols $\mathcal{F}_G$, $\mathcal{W}_{nG}$, and $\mathcal{W}_{nmG}$, which we use from now on, have the same definition already given in (67) and (73), with the substitution of v with v_G only in the exponential term.

We are now ready to evaluate the quantum moments by applying the rules (81) and (82) to Eqs. (54). For the zeroth moment we have

$$\langle(\hat{u}_{i+p}-\hat{u}_i)^2\rangle=\langle(u_{i+p}-u_i)^2\rangle_G+\sum_{k'}U_{k'l}U_{k'j}(\alpha_{k'}+\langle\delta\alpha_{k'}\rangle_G)(\delta_{l,i+p}\delta_{j,i+p}+\delta_{l,i}\delta_{j,i}-\delta_{l,i}\delta_{j,i+p}-\delta_{l,i+p}\delta_{j,i}) =p\left[\frac{\mathcal{F}_G''(s_0)}{\mathcal{F}_G(s_0)}-a^2\right]+\frac{2}{N}\sum_{k'}\left[\alpha_{k'}+\frac{\omega_{k'}}{2}\frac{\partial\alpha_{k'}}{\partial\omega_{k'}}\left[\frac{\mathcal{W}_{2G}-v''(a)}{\tilde{v}''(a)}\right]\right][1-\cos(pk'a)]\,, \quad (85)$$

and the final result when $k \neq 0$ is

$$\mu_0^Q(k) = -4\pi \left[\left[\frac{\mathcal{F}_G''(s_0)}{\mathcal{F}_G(s_0)} - a^2 \right] \frac{1}{4\sin^2(ka/2)} + \alpha_k + \frac{\omega_k}{2} \frac{\partial \alpha_k}{\partial \omega_k} \left[\frac{\mathcal{W}_{2G} - v''(a)}{\bar{v}''(a)} \right] \right] . \tag{86}$$

To evaluate the quantum second moment, we start from $\langle \hat{p}_{i+p} \hat{p}_i \rangle$ and apply Eq. (82). By using the relation

$$\frac{\partial \gamma_k}{\partial \omega_k} = m^2 \left[2\omega_k \alpha_k + \omega_k^2 \frac{\partial \alpha_k}{\partial \omega_k} \right] , \tag{87}$$

we easily obtain

$$\mu_2^Q(k) = -4\pi \left[\frac{k_B T}{m} + \omega_k^2 \alpha_k + \omega_k^2 \left[\alpha_k + \frac{\omega_k}{2} \frac{\partial \alpha_k}{\partial \omega_k} \right] \left[\frac{\mathcal{W}_{2G} - v''(a)}{\bar{v}''(a)} \right] \right] . \tag{88}$$

The application of Eq. (81) to the evaluation of the quantity $\langle \hat{V}_{i+p} \hat{V}_i \rangle$ which appears in the fourth moment gives a term which is equal to the classical one, but for the substitution of the classical average with the G average, and in addition a correction term, which, after some algebra, in the LCA approximation scheme can be written

$$\begin{aligned} \frac{1}{2} \sum_{ij} \left\langle (\alpha_{lj} + \delta\alpha_{lj}) \frac{\partial^2}{\partial u_l \partial u_j} \left[\frac{\partial V}{\partial u_{i+p}} \frac{\partial V}{\partial u_i} \right] \right\rangle_G &= \mathcal{D}(\mathcal{W}_{13G} - \mathcal{W}_{1G}\mathcal{W}_{3G})(2\delta_{p,0} - \delta_{p,1} - \delta_{p,-1}) \\ &+ (6D_p - 4D_{p-1} - 4D_{p+1} + D_{p-2} + D_{p+2})\{[\bar{v}''(a)]^2 + 2\bar{v}''(a)[\mathcal{W}_{2G} - v''(a)]\} \\ &+ (6\langle \delta D_p \rangle_G - 4\langle \delta D_{p-1} \rangle_G - 4\langle \delta D_{p+1} \rangle_G \\ &+ \langle \delta D_{p-2} \rangle_G + \langle \delta D_{p+2} \rangle_G)[\bar{v}''(a)]^2 , \end{aligned} \tag{89}$$

where we have defined $\delta D_p = \sum_k U_{i,k} U_{i+p,k} \delta\alpha_k$. By Fourier transforming the previous expression, and combining with the results (74) and (77), we have

$$\begin{aligned} \mu_4^Q(k) = -\frac{4\pi}{m^2} \Bigg[&(\mathcal{W}_{11G} - \mathcal{W}_{1G}^2) + \mathcal{D}(\mathcal{W}_{13G} - \mathcal{W}_{1G}\mathcal{W}_{3G}) \\ &+ m\omega_k^2 \left\{ \left[\alpha_k + \frac{\omega_k}{2} \frac{\partial \alpha_k}{\partial \omega_k} \left[\frac{\mathcal{W}_{2G} - v''(a)}{\bar{v}''(a)} \right] \right] \bar{v}''(a) + 2\alpha_k [\mathcal{W}_{2G} - v''(a)] \right\} \Bigg] 4\sin^2 \left[\frac{ka}{2} \right] . \end{aligned} \tag{90}$$

Remembering expression (64) for the LCA effective potential v_G and approximating to first order in $\mathcal{D}$, by partial integration we have

$$\begin{aligned} \mathcal{W}_{1G} &= -s_0 k_B T - \frac{\mathcal{D}}{2} \mathcal{W}_{3G} , \\ \mathcal{W}_{11G} &= k_B T \mathcal{W}_{2G} - s_0 k_B T \mathcal{W}_{1G} - \frac{\mathcal{D}}{2} \mathcal{W}_{13G} , \\ \mathcal{W}_{13G} &= k_B T \mathcal{W}_{4G} - s_0 k_B T \mathcal{W}_{3G} = \frac{\mathcal{D}}{2} \mathcal{W}_{33G} , \end{aligned} \tag{91}$$

so that, at first order in $\mathcal{D}$,

$$(\mathcal{W}_{11G} - \mathcal{W}_{1G}^2) + \mathcal{D}(\mathcal{W}_{13G} - \mathcal{W}_{1G}\mathcal{W}_{3G}) \simeq k_B T \left[\mathcal{W}_{2G} + \frac{\mathcal{D}}{2} \mathcal{W}_{4G} \right] . \tag{92}$$

The final result for the LCA quantum fourth moment is therefore

$$\begin{aligned} \mu_4^Q(i) = -4\pi\omega_k^2 \Bigg[&\frac{k_B T}{m} \left[\mathcal{W}_{2G} + \frac{\mathcal{D}}{2} v^{IV}(a) \right] \frac{1}{\bar{v}''(a)} + \omega_k^2 \alpha_k \\ &+ \omega_k^2 \left[2\alpha_k + \frac{\omega_k}{2} \frac{\partial \alpha_k}{\partial \omega_k} \right] \left[\frac{\mathcal{W}_{2G} - v''(a)}{\bar{v}''(a)} \right] + \frac{k_B T}{m} \frac{\mathcal{D}}{2} \left[\frac{\mathcal{W}_{4G} - v^{IV}(a)}{\bar{v}''(a)} \right] \Bigg] . \end{aligned} \tag{93}$$

In the calculation of the quantum sixth moment new terms having a quantum origin are present from the very beginning. Indeed, Eq. (58) is replaced by (54). By applying Eq. (36), however, many terms cancel each other and the result we get is

$$\left\langle \frac{d^3\hat{u}_{i+p}}{dt^3}\frac{d^3\hat{u}_i}{dt^3}\right\rangle = \frac{1}{m^4}\sum_{jj'}\left\langle\left\langle \frac{\partial^2 V}{\partial u_{i+p}\partial u_j}\frac{\partial^2 V}{\partial u_i \partial u_{j'}}\right\rangle_{\mathbf{x}}[mk_BT\delta_{jj'}+\gamma_{jj'}(\mathbf{x})]\right\rangle_G + \frac{\hbar^2}{4m^4}\sum_{jj'}\left\langle\left\langle \frac{\partial^3 V}{\partial u_{i+p}\partial u_j \partial u_{j'}}\frac{\partial^3 V}{\partial u_i \partial u_j \partial u_{j'}}\right\rangle_{\mathbf{x}}\right\rangle_G , \tag{94}$$

and the last term can also be dropped in the LCA because it is of order $\hbar^2\sim\alpha^2$. From Eq. (82) we can therefore conclude that, in LCA,

$$\left\langle \frac{d^3\hat{u}_{i+p}}{dt^3}\frac{d^3\hat{u}_i}{dt^3}\right\rangle = \frac{k_BT}{m^3}\sum_j\left\langle \frac{\partial^2 V}{\partial u_{i+p}\partial u_j}\frac{\partial^2 V}{\partial u_i\partial u_j}\right\rangle_G + \frac{k_BT}{2m^3}\sum_j\sum_{ll'}\left\langle \frac{\partial^2}{\partial u_l \partial u_{l'}}\left[\frac{\partial^2 V}{\partial u_{i+p}\partial x_j}\frac{\partial^2 V}{\partial u_i \partial u_{j'}}\right](\alpha_{ll'}+\delta\alpha_{ll'})\right\rangle_G + \frac{1}{m^4}\sum_{jj'}\left\langle\left[\frac{\partial^2 V}{\partial x_{i+p}\partial x_j}\frac{\partial^2 V}{\partial u_i\partial u_{j'}}\right](\gamma_{jj'}+\delta\gamma_{jj'})\right\rangle_G . \tag{95}$$

Now we observe that the first term in the last expression parallels with the classical one, while the last term, if $\gamma_{jj'}$ is changed to $\alpha_{jj'}$, has the same form as the terms proportional to the second derivative of the potential in Eq. (89), so that the results obtained before can be used. The evaluation of the second term is more lengthy but straightforward, so we will omit the details of the calculation. At the end, the LCA quantum sixth moment comes out to be

$$\begin{aligned}\mu_6^Q(k) = -4\pi\Bigg\{ &\frac{k_BT}{m^3}\Bigg\{[\mathcal{W}_{2G}^2+\bar{v}''(a)v^{IV}(a)\mathcal{D}-\tfrac{1}{2}v'''(a)^2(\mathcal{D}-\bar{\mathcal{D}})]\frac{m^2}{\bar{v}''(a)^2}\omega_k^4 \\ &+[2(\mathcal{W}_{22G}-\mathcal{W}_{2G}^2)+v'''(a)^2(3\mathcal{D}-\bar{\mathcal{D}})]\frac{m}{\bar{v}''(a)}\omega_k^2\Bigg\} \\ &+\omega_k^6\alpha_k+\omega_k^6\left[3\alpha_k+\frac{\omega_k}{2}\frac{\partial\alpha_k}{\partial\omega_k}\right]\left[\frac{\mathcal{W}_{2G}-v''(a)}{\bar{v}''(a)}\right] \\ &+\frac{k_BT}{m^2}\omega_k^2\left[\frac{v'''(a)^2}{\bar{v}''(a)}(3\delta\mathcal{D}-\delta\bar{\mathcal{D}})+m\omega_k^2\left[\frac{v^{IV}(a)}{\bar{v}''(a)}(\mathcal{D}+\delta\mathcal{D})-\frac{v'''(a)^2}{2\bar{v}''(a)^2}(\delta\mathcal{D}-\delta\bar{\mathcal{D}})\right]\right] \\ &\times\left[\frac{\mathcal{W}_{2G}-v''(a)}{\bar{v}''(a)}\right]+\frac{2k_BT}{m^2}\omega_k^2\left[v'''(a)\left[3\mathcal{D}-\bar{\mathcal{D}}-\frac{\mathcal{D}-\bar{\mathcal{D}}}{2}\frac{m\omega_k^2}{\bar{v}''(a)}\right]\right]\left[\frac{\mathcal{W}_{3G}-v'''(a)}{\bar{v}''(a)}\right]\Bigg\},\end{aligned} \tag{96}$$

where we have defined the new quantities

$$\delta\mathcal{D}=\frac{1}{N}\sum_k 4\sin^2\left[\frac{ka}{2}\right]\frac{\omega_k}{2}\frac{\partial\alpha_k}{\partial\omega_k}, \qquad \delta\bar{\mathcal{D}}=\frac{1}{N}\sum_k 4\sin^2\left[\frac{ka}{2}\right]\left[\cos^2\left[\frac{ka}{2}\right]-1\right]\frac{\omega_k}{2}\frac{\partial\alpha_k}{\partial\omega_k}. \tag{97}$$

VI. APPLICATION TO THE LENNARD-JONES CHAIN

In this section the formalism developed above is applied to the Lennard-Jones chain, whose interaction potential has the form given in Eq. (44), with

$$v(r)=4\epsilon\left[\left[\frac{\sigma}{r}\right]^{12}-\left[\frac{\sigma}{r}\right]^{6}\right]. \tag{98}$$

In the numerical computation, appropriate units defined as function of the constants m, σ, and ϵ have been used. The reduced temperature is defined as $t=k_BT/\epsilon$, the frequency is measured in units $\bar{\omega}=\sqrt{\epsilon/m\sigma^2}$, and the moment μ_{2n} is given in units $\bar{\omega}^{2n}\sigma^2$. All the explicit results given below have been obtained by setting the average distance a between two NN atoms at the value $a=L/N=r_0\equiv\sigma^6\sqrt{2}$, which corresponds to the position of the minimum of the potential (98). In the quantum calculation, the quantum coupling parameter

$$\lambda=\{[\hbar^2v''(r_0)]/(m\epsilon\sigma^2)\}^{1/2}$$

has been fixed to the value $\lambda=0.23$, obtained using the characteristic interaction parameters of argon.

A. Numerical evaluation of the moments by effective potential

The evaluation of the classical moments reduces to the computation of the quantities $\mathcal{T}$ and $\mathcal{W}$ which appear in the expressions for the moments obtained in Sec. V. Such computation can be made in an analytic way only for very simple interaction potentials and it has to be done numerically for the Lennard-Jones (LJ) one. It has actually been performed by using standard double precision FORTRAN routines, requiring a relative precision of 10^{-10} in the evaluation of the integrals (67) and (73) and in the solution of the implicit equation (68) for s_0. In the quantum regime we also need the renormalization parameters $\mathcal{D}$ and $\bar{\mathcal{D}}$ and the corresponding corrections $\delta\mathcal{D}$ and $\delta\bar{\mathcal{D}}$. They have been computed in a self-consistent way by following the procedure used in Ref. 10. We point out that any calculation of quantum moments by means of the

effective potential requires only few seconds of numerical computation on a personal computer; that is, a time of the same order of magnitude of that required in the classical case.

B. Evaluation of moments by Monte Carlo simulation

The evaluation of both the classical moments given by Eqs. (58) through Eq. (55), and the quantum moments given by Eqs. (54) through Eqs. (11)–(13) is based on Metropolis sampling techniques. Metropolis sampling techniques are standardly used in classical MC problems, and it is the mapping presented in Sec. II B of the quantum-mechanical averages into expressions involving classical configuration integrals which allows us to apply these Metropolis techniques to evaluate the moments of the quantum-mechanical spectral density. One can appreciate the increased complexity in the evaluation of the thermodynamics of our N-atom (or N-variable) quantum-mechanical chain over that for the evaluation of the N-atom classical chain by considering that the thermodynamic averages of the N-atom one-dimensional quantum system are rewritten in Sec. II B as configuration integrals for a two-dimensional system with $N\times P$ classical variables. In the following we shall first describe how Metropolis sampling was applied to the N-atom classical chain and then how these sampling techniques were applied to the discretized path-integral expressions for the moments of the quantum-mechanical spectral density.

1. Classical regime

In the MC evaluation of the expressions in Eqs. (55) for the moments of the classical spectral density of the nearest-neighbor LJ chain, we have considered a chain with $N=40$ atoms for $ka=\pi/5,\frac{3}{5}\pi,\pi$ and $k_BT/\epsilon=0.2,0.3,0.4$. As we shall see below, there is good agreement between these MC results for $N=40$ and the exact $N\to\infty$ results obtained analytically in Sec. V A for $ka=\frac{3}{5}\pi$ and $ka=\pi$. The poorest agreement is found for the lowest wave vector and the sixth moments, but this is to be expected because finite-size effects become more important in lowering the wave vector and increasing the order of moments.

In the Metropolis sampling technique, we generate 1.6×10^8 atomic configurations which are used to compute thermodynamic averages. These configurations are generated by using a selection process in which the program statistically generates test atomic configurations for the system and then applies a criterion to determine whether or not each generated configuration will be accepted or rejected. The program is set up to generate and check one random test configuration at a time, and in our simulations the acceptance ratio is between 40 and 60%. In the sampling process, a test configuration is generated by (a) first taking the current N-atom configuration of the system and choosing an atom to move (the atom to be moved was chosen sequentially on the chain); (b) the chosen atom is then given a new position on the chain. The new position of the atom is obtained by choosing a random number between $-\bar{x}$ and $\bar{x}$ for some fixed value of $\bar{x}$ and adding this randomly chosen number to the original position of the atom.

The values of $\bar{x}$ is fixed during the course of the simulation to obtain the 40–60% acceptance of new configurations into the set of the 1.6×10^8 configurations used to compute averages. For the temperatures we consider, $\bar{x}/a\simeq0.11$, so that the atoms are effectively restricted to maintain their sequential order on the chain.

During the course of the simulation, values of the first four classical even moments were printed out after every 8×10^6 configurations. The error in the final printed out values of the moments at the end of the program was then estimated as the average of the absolute difference between the last printed out moment and its previous four or five printed out values.

2. Quantum regime

The simulation for the quantum moments, expressed by Eqs. (11)–(13) as configuration integrals involving classical variables $\{x_i(l)\}$, is based on a similar Metropolis sampling method, but now for a system of $N\times P$ variables defined in two dimensions. For the quantum simulation we have taken $N=20,40$ and $P=4,8,16$, where $P=16$ is believed from previous work[31] to give an accurate representation of the $P\to\infty$ limit. The total number of configurations used in computing the final average moments at the end of the programs was 2×10^7, with average moments printed out every 10^6 configurations.

As with the classical MC discussed above, new configurations for the Metropolis sampling of our quantum path integrals are generated by moving sequentially through the $\{x_i(l)\}$ variables of the $N\times P$ lattice, and choosing at each sampling an $x_i(l)$ to receive a random increment. The random addition to $x_i(l)$ is taken from the interval $-\bar{x}$ to $\bar{x}$, with $\bar{x}$ chosen to assure a 40–60% acceptance rate for the newly generated configurations. In choosing new configurations $\bar{x}/a\simeq0.1$ and the atoms are again not allowed to change their sequential ordering on the chain.

Quantum simulation runs were made for the first three even moments of the quantum spectral density at $k_BT/\epsilon=0.1,0.2,0.3$ and $ka=\pi/5,\pi/2,\pi$. As we shall see below, good agreement of the quantum simulation moments with those obtained by means of variational calculations is observed for the highest wave vectors. For $ka=\pi/5$, the finite-size effects prevent us from having quantitative comparison between $N=40$ and ∞ chains; however, an overall agreement is obtained. As long runs are required to assure the accuracy of the QMC results, it is difficult to obtain numerous independent runs due to the limitations of computer time. In light of this fact, we have computed the errors in the final simulation values of the quantum moments as being the deviations, found in the last ten incremental steps of 10^6 configurations printed out during the course of the QMC program, from the final values given by the simulation.

Also, if $P=16$ can be believed to give a good estimate of the $P\to\infty$ limit, following the standard procedure, we have plotted our QMC results for the moments, obtained

for a low Trotter number ($P=4,8,16$), against $1/P$, in order to extrapolate the data to $P=\infty$. A quadratic extrapolation has been used for all data sets, but, given the error bars, a linear extrapolation would have been equally appropriate for some of them. In analyzing the QMC data, we have also applied a simple expedient described in Ref. 12. It consists of adding to the computed quantities the difference between the exact quantum value and the finite Trotter number result for the same quantity in the harmonic approximation. Such a device has been revealed to be very efficient in improving the convergence of QMC data to the $P=\infty$ value at the lowest temperature, especially for the zeroth and the second moment. An example of such procedure is reported in Fig. 1.

C. Results and discussion

The results we obtained for the frequency moments of the spectral density (45) of a Lennard-Jones chain are summarized in Figs. 2–5, where the temperature dependence of the first four classical and quantum even moments is shown for three different wave vectors (note that, with our definition, all the moments are negative, so that their absolute value is reported in the figures). For the sixth moments, only the classical MC data are available because the evaluation of the quantum ones with a tolerable error would require too long simulation times. On the other hand, the QMC data are not really essential, once the reliability of the results of the effective potential method has been ascertained in the range where finite-

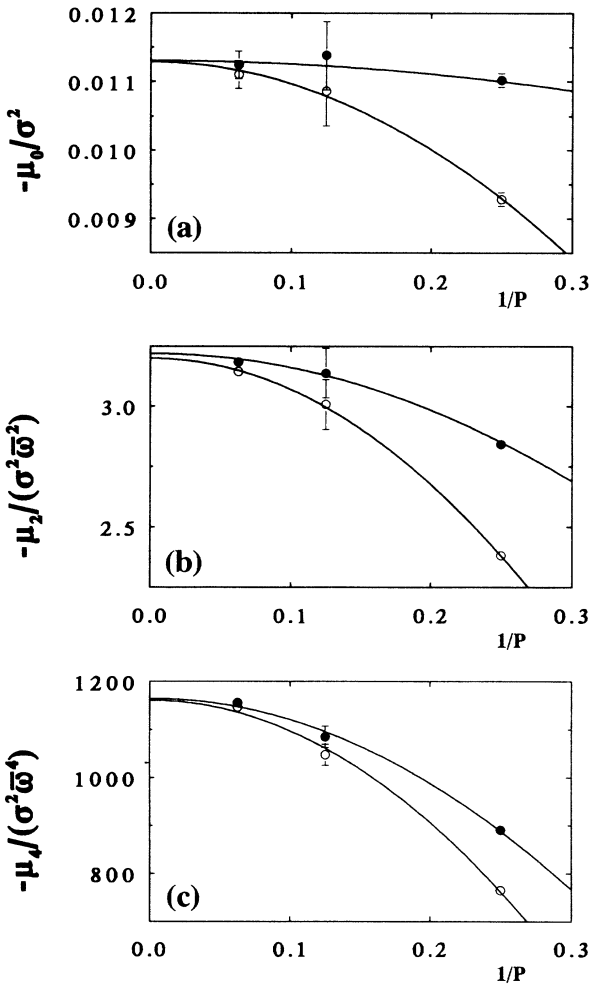

FIG. 1. Quantum Monte Carlo results for the moments (a) μ_0, (b) μ_2, and (c) μ_4 of the 20-atom chain, for quantum coupling $\lambda=0.23$, at $t=0.1$ and for $ka=\pi$ are reported vs the inverse Trotter number $1/P$. The open circles are the raw results of the QMC simulations, while the solid circles are the same data corrected for the finite Trotter number effects onto the harmonic contribution, as explained in the text. The lines are the fitted parabolas.

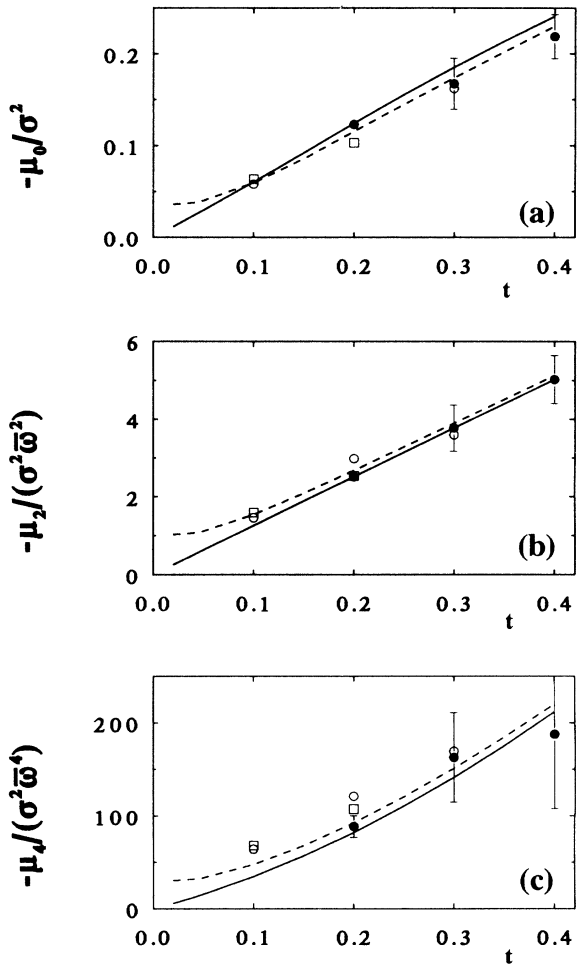

FIG. 2. Moments (a) μ_0, (b) μ_2, and (c) μ_4 for $ka=\pi/5$ vs the reduced temperature t (see text). The solid line is the classical result, the dashed line the quantum effective potential result, while the symbols are the classical and quantum Monte Carlo data. The quantum results refer to $\lambda=0.23$. The classical MC data (solid circles) are those obtained for a chain of 40 atoms, while the QMC data are the results for a chain of 20 atoms (open circles) and 40 atoms (open squares). μ_0 is measured in units of σ^2, μ_2 in units of $\sigma^2\bar{\omega}^2$, and μ_4 in units of $\sigma^2\bar{\omega}^4$ (the parameters σ and $\bar{\omega}$ are defined in Sec. VI). Note that all the moments are negative.

size effects do not play an important role. In Fig. 5 we report the sixth moment only for $ka=\pi$; indeed the behavior of this quantity for the other wave vectors is very similar.

Just by observing the figures, it appears that the classical MC data reproduce very well many analytical results for the classical moments. Moreover, the effective potential clearly accounts for the quantum effects at low temperature and, as it is implicit in the method, it correctly approaches the classical behavior at high temperature. It can be verified very easily that, at very low temperature, the effective potential reproduces the results given by the self-consistent harmonic approximation, but at intermediate temperatures it also accounts for the leading quantum effects of nonlinearity.

About the comparison between the QMC data and the effective potential results, we can conclude that the overall agreement is certainly very good for the zeroth and the second moment, while for the fourth moment the situation is a little bit less favorable, especially for the lowest wave vector. In fact, we see that, for all three wave vectors, the QMC values for the fourth moments are higher than those obtained by the effective potential, but while the differences at the zone boundary are minimal, they become more apparent for the smallest wave vector. We attribute this partial disagreement between QMC and effective potential results to the finite length of the chain used in QMC simulations. Finite-size effects indeed become more important for longer wavelengths; moreover we expect that they affect more the highest moments because, as can be seen from Eqs. (54), (72), and (78), every elementary contribution to the moments is given by a cluster of particles which becomes larger as the order of the moments increases.

VII. DYNAMICAL RESPONSE FUNCTION OF A QUANTUM CHAIN

The effective potential has been defined for the evaluation of static quantities. The partition function can be directly calculated, while the static correlations have been calculated taking into account their Gaussian quantum spread. Of course, it is apparently meaningless to try to extract dynamical information from the effective potential by using it, for instance, as the interaction potential in molecular-dynamics simulations, as was suggested in Refs. 32 and 33. However, starting from the knowledge of the frequency moments, a reconstruction of the function $C(k,\omega)$ itself can be devised.

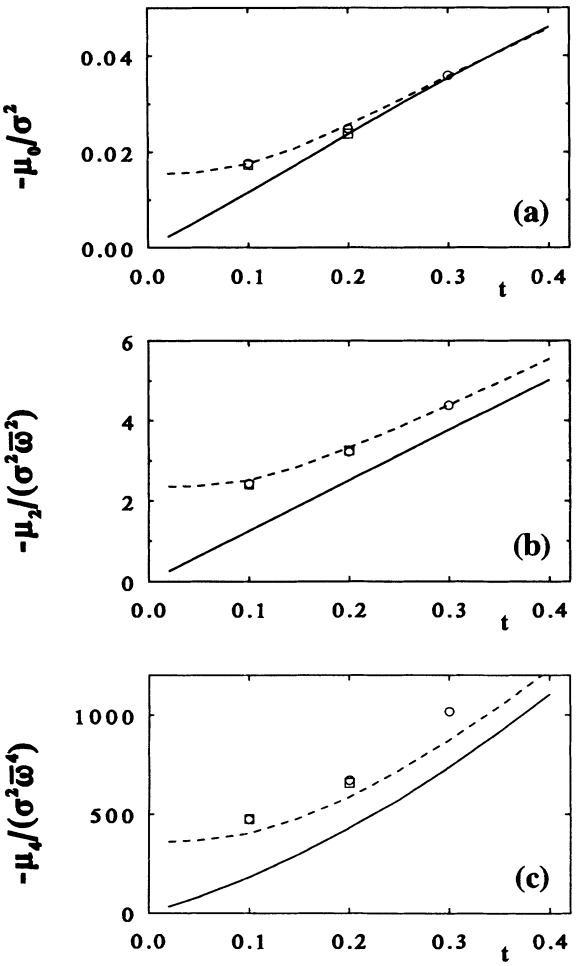

FIG. 3. The same as in Fig. 2, for $ka=\pi/2$.

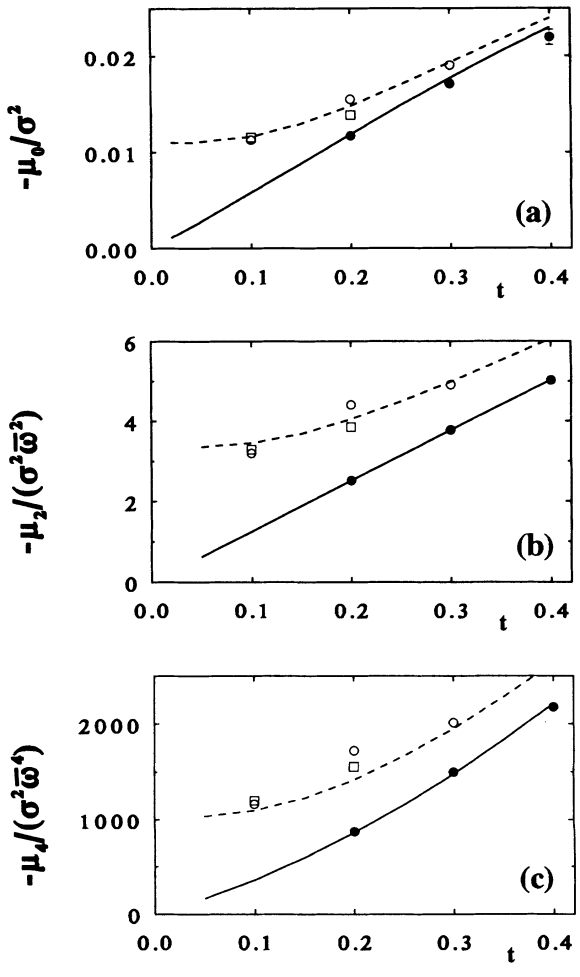

FIG. 4. The same as in Fig. 2, for $ka=\pi$.

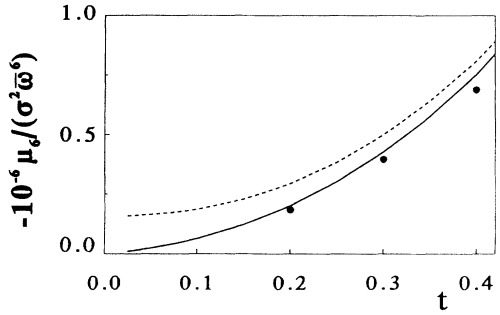

FIG. 5. Classical and quantum sixth moment, μ_6, as a function of the reduced temperature t for $ka=\pi$. The symbols have the same meaning as in Fig. 2.

We start from the continued fraction expansion proposed by Mori.[34,17] The function $C(k,\omega)$, admits the following continued fraction representation:

$$C(k,\omega)=\mu_0(k)\cdot\mathrm{Re}\left[\frac{1}{\pi}\cdot\cfrac{1}{z+\cfrac{\delta_1}{z+\cfrac{\delta_2}{z+\cdots}}}\right]_{z=i\omega}$$
$$\equiv\mu_0(k)F(k,\omega)\ , \tag{99}$$

where we have defined the normalized function $F(k,\omega)=\mathrm{Re}[\psi(k,i\omega)]$, which has the same ω dependence of $C(k,\omega)$, and denoted with ψ the complex function of z within the squared brackets. The expansion coefficients δ_n are related to the frequency moments by algebraic relations. The explicit expressions for the first three of them are

$$\delta_1=\frac{\mu_2}{\mu_0}\ ,$$
$$\delta_2=\frac{\mu_4}{\mu_2}-\frac{\mu_2}{\mu_0}\ , \tag{100}$$
$$\delta_3=\frac{1}{\delta_2}\left[\frac{\mu_6}{\mu_2}-\left[\frac{\mu_4}{\mu_2}\right]^2\right]\ .$$

Since these static quantities can be evaluated by means of the effective potential, this scheme appears to offer a tool to calculate quantum-dynamical correlations.

In the harmonic approximation, δ_n vanish for $n>1$. For weakly anharmonic systems, the knowledge of the first δ-s allows one to reproduce the spectral shape with sufficient accuracy, by introducing reasonable termination criteria for the expansion (99). This corresponds to introduce finite lifetimes of the elementary excitations, as done by second-order expansions of the phonon self-energy. By making some assumptions on the physical processes which are responsible for the determination of the line shape, the method can also be extended to other regimes which are not nearly harmonic.[35]

However, some cautions are in order. First we note that $\delta_2,\delta_3,\ldots,\delta_n$ often are relatively small quantities. Their evaluation, as is clear from Eqs. (100) involves subtractions between terms which can be very large. Therefore, high precision is required in the computation of the moments $\mu_{2n}(k)$, otherwise the belief that the evaluation of higher-order moments surely leads to an improvement in the reconstruction of the spectral shape is illusory. Moreover, higher-order moments require higher-order static correlations which can be obtained with decreasing reliability from the numerical calculations. Finally, the continued fraction expansion is poorly convergent for strongly anharmonic systems, and the choice of the termination is a source of arbitrariness in reconstructing the spectral shape.

Among various recipes proposed in order to truncate the continued fraction expansion, we recall here the Gaussian termination,[19,20] and the three-pole approximation.[18] The latter can be easily extended to higher order to become an n-pole approximation. Both of them can be better introduced if we rewrite $\psi(x)$ in the iterated form:

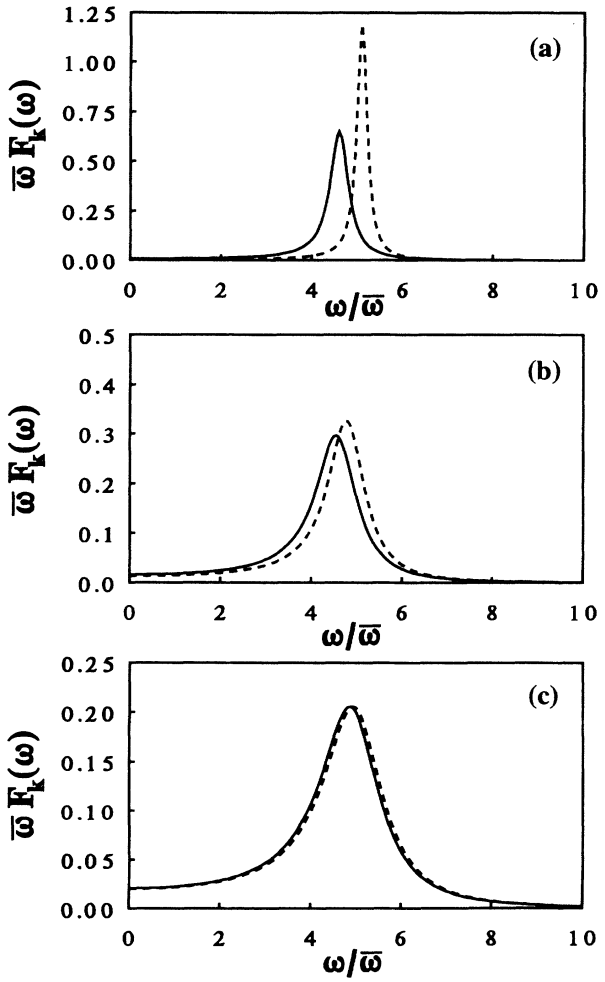

FIG. 6. Normalized response function $F_k(\omega)$ for $ka=\pi/5$ at the temperatures (a) $t=0.1$, (b) $t=0.3$, and (c) $t=0.8$. The solid line is the classical result, while the dashed line is the quantum result (the characteristic frequency $\bar{\omega}$ is defined in Sec. VI).

$$\psi(z)=\frac{1}{\pi}\frac{1}{z+\delta_1\psi_1(z)}\ ,$$
$$\psi_n(z)=\frac{1}{z+\delta_{n+1}\psi_{n+1}(z)}\ . \tag{101}$$

In the Gaussian approximation at the nth order, the expansion (99) is truncated by setting $\psi_n(z)$ equal to the Laplace transform of a Gaussian with variance δ_{n+1}:

$$\psi_n(z)=\left[\frac{\pi}{2\delta_{n+1}}\right]^{1/2} e^{z^2/2\delta_{n+1}} \times\left[1-\frac{2}{\sqrt{\pi}}\int_0^{z/\sqrt{2\delta_{n+1}}} e^{-x^2}dx\right]\ . \tag{102}$$

In the n-pole approximation $\delta_n\psi_n(z)$ is more simply approximated by a constant value $1/\tau=\delta_n\psi_n(0)$, which is determined assuming again a functional dependence like (102) for ψ_n or for ψ_{n-2}. In the first case we have $1/\tau=\delta_n\sqrt{\pi/2\delta_{n+1}}$, while in the second $1/\tau=\sqrt{\pi\delta_{n-1}/2}$, so that the number of parameters δ-s to be determined is reduced by two.

In Figs. 6–8, the function $F(k,\omega)$ for the Lennard-Jones chain is shown at three different temperatures and three different wave vectors; the continuous and dashed lines refer, respectively, to the classical and quantum results. The Gaussian termination at third order has been applied, and the parameters δ have been deduced from the values of the moments obtained in the previous section, using, in the quantum regime, the results given by the effective potential method. The modification of the line shape due to the quantum effects is apparent. The shift of the peak position, related to the frequency renormalization due to the quantum fluctuations, and the different width of the peak are two important features. If an n-pole approximation is used, both the classical and quantum line shapes change a little, but the relative changes in shape are essentially the same already obtained with the Gaussian termination.

At the actual stage, there is no underlying physical reason to rigorously justify these truncation criteria for the Lennard-Jones chain, so that the reliability of the line shapes obtained may be somehow questionable. However, this problem is not peculiar of the quantum regime, since it is already present in the study of the classical system. The overall meaning of the present work is therefore clear. As a significant issue, we have shown how quantum effects can be easily taken into account, also for

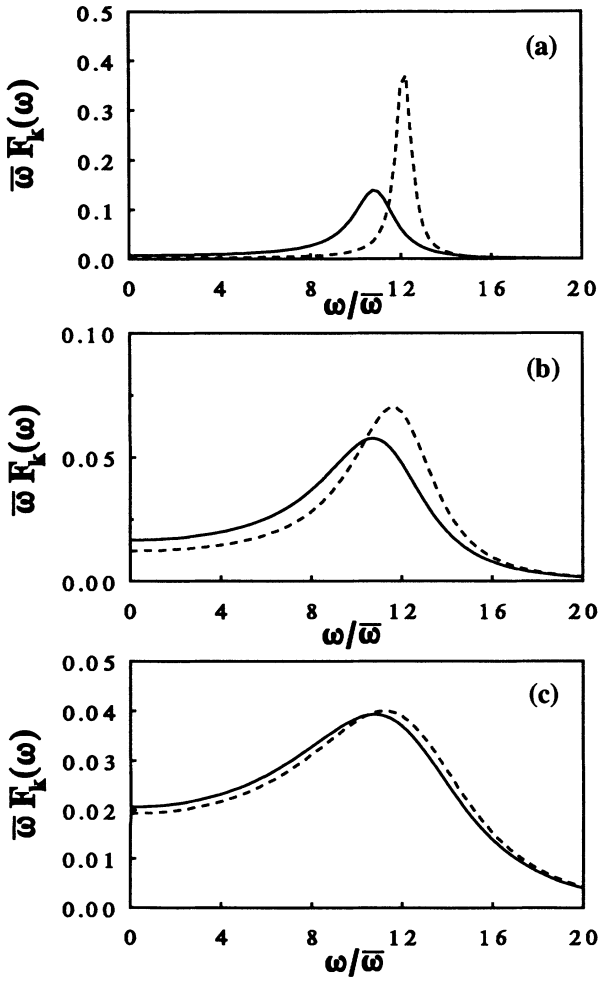

FIG. 7. The same as in Fig. 6, for $ka=\pi/2$.

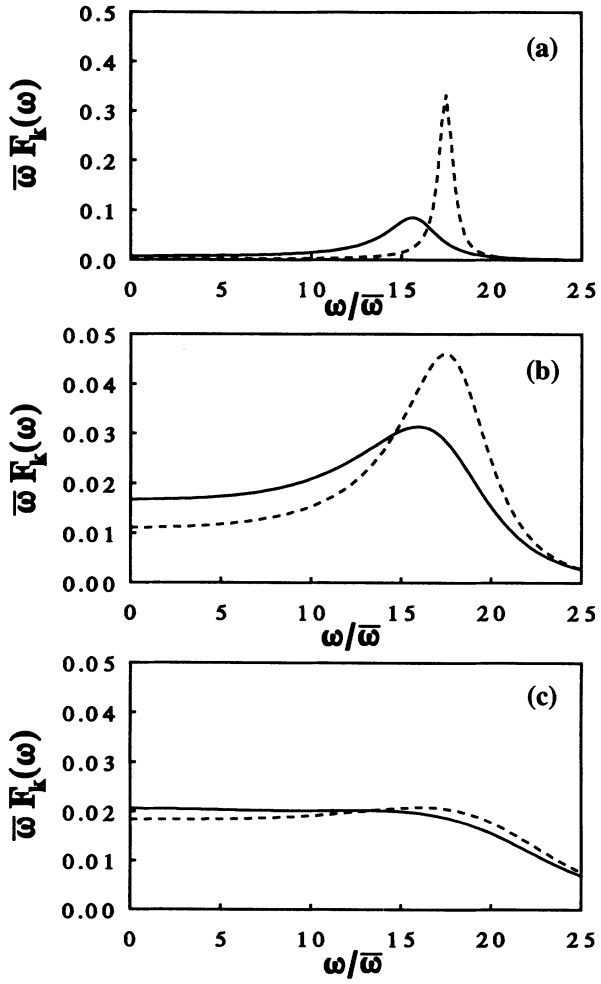

FIG. 8. The same as in Fig. 6, for $ka=\pi$.

studying dynamical properties. We have presented an approach which reduces quantum calculations to classical ones, so that every progress in the determination of the response function of a classical system starting from static quantities can be usefully transferred to the quantum regime.

VIII. SUMMARY AND CONCLUSIONS

We have investigated the properties of the time-dependent displacement correlation functions of a one-dimensional chain of atoms. This was done by (1) computing the frequency moments of the spectral densities of the time-dependent displacement correlation functions using analytical, numerical, and Monte Carlo simulation techniques, and (2) using the best values of the moments obtained in (1) to develop a continued fraction representation of the spectral densities of the time-dependent correlation functions, based on theories of Refs. 17, 19, 20, and 34 for these representations. Both quantum and classical models of the one-dimensional chain were studied, and comparisons of the quantum and classical moments and spectral densities were made.

We have chosen for our studies time-dependent displacement correlation functions which are related to the cross sections for the inelastic scattering of neutrons from our vibrational systems. The spectral representations of these correlation functions in the harmonic approximation are sums of simple poles and hence are exactly representable in terms of continued fraction expansions of finite length. In the presence of weak anharmonicity, it has been our expectation that the infinite continued fraction representations of the spectral densities of the same correlations functions for the now fully anharmonic system will yield accurate spectral densities for some approximate termination scheme applied to the continued fraction. We believe that our results presented in Figs. 6–8 represent, to varying degrees, such accurate representations by artificially terminated continued fractions of the spectral densities of the fully anharmonic Lennard-Jones chain as functions of temperature and wave number. In particular, we expect that the spectral densities in Figs. 6–8 which differ the most from the pole structures of the spectral densities calculated in the harmonic approximations are least likely to provide accurate representations of the true spectral densities of the anharmonic system which they are intended to portray. We feel that such representations which differ significantly from those of the harmonic approximation are most likely to depend on the termination scheme applied in developing the continued fraction representation. In Figs. 6–8, they appear to reconstruct the spectral representations of our chain of atoms best for $t \leq 0.3$ and for $ka < \pi$.

In computing the moments of the spectral densities a number of analytical and MC computer simulation techniques were used. A comparison of the moments computed by these various techniques was made to assure the accuracy of the moments used in the continued fraction representations whose results are presented in Figs. 6–8. Figures 2–4 present the moments computed for the classical and quantum atomic chains. The classical moments were obtained analytically using an extension of the Gürsey method, and were compared with the results of a classical MC simulation for a system of 40 atoms subject to periodic boundary conditions. The agreement between the results of these two classical methods is good, in general, and is best for wave vectors at the edge of the Brillouin zone. In the computation of the quantum moments, the effective potential method was compared to the results from the QMC method for these same moments. For the QMC moments an illustration of the effects of a finite P was given in Fig. 1, where a polynomial fit was used to extract the $P \rightarrow \infty$ limits of these moments. In Figs. 2–4 the corrected QMC moments and the effective potential results for these moments were found to agree well with one another. The poorest agreement between the results from the two quantum-mechanical approaches was found for $ka = \pi/5$ at $t = 0.3$. Consequently, we have used the quantum-mechanical moments computed by means of the effective potential method to obtain the continued fraction representation in Figs. 6–8.

In general, we have found that both the classical and QMC moments exhibit the greatest deviations from their counterparts obtained by analytical means for the higher moments, e.g., μ_4, and for the moments evaluated at long wavelengths. This is most likely due to the finite number of atoms used in the simulation methodologies. The higher-order moments of the spectral densities and the moments of the spectral densities computed for long wavelengths are dependent on the motion of more of the atoms along the chain than are the lower-order moments for shorter wavelengths. These finite-size effects (in the number of atoms) are another reason we have chosen the effective potential and extended Gürsey classical moments in developing the continued fraction results presented in Figs. 6–8.

Looking at the results presented in Figs. 6–8 for the classical and quantum-mechanical spectral densities at $t = 0.1$, 0.3, and 0.8, we see that, at low temperatures ($t \leq 0.3$), the classical and quantum spectral densities are quite different. The peak in the quantum-mechanical spectral density occurs at higher frequencies than that in the corresponding classical spectral density, and the quantum peaks are generally narrower than that in the corresponding classical system. We remember that both quantum and classical results have been obtained taking the same, fixed chain spacing; this explains why the shift of the peak is towards the higher frequencies. About the narrowing of the quantum peaks from their classical counterparts, a possible explanation may reside in coherent effects arising from the wave nature of quantum particles. This coherence may correlate the motions of the particles in the system, decreasing their collisions and subsequently increasing the lifetimes of the quasiexcitations in the system. The low-temperature motion of the classical and quantum particles in these chains are certainly quite different, as the difference in peak energy in the classical and corresponding quantum system indicates that different parts of the Lennard-Jones potentials must be sampled in the two different systems.

In conclusion, we see that the spectral densities at low temperatures of the nonlinear chain of atoms can be well represented by continued fraction expansions based on the moments of the spectral density. We expect that these methods should be even more successful when they are applied to the low-temperature properties of higher-dimensional systems. These systems are less susceptible to fluctuations than are the one-dimensional systems we have considered in this paper, and should have well-defined quasiexcitation peaks in their spectral densities. The extension of these methods to three-dimensional vibrational systems is now in progress.

ACKNOWLEDGMENTS

A.A.M. and A.R.M. would like to thank the Dipartimento di Fisica dell'Università di Firenze for its hospitality while a major portion of their contribution to the work was carried out. The work of A.A.M. was supported in part by NSF Grant No. 89-18184. It was also supported by the University of California, Irvine, through an allocation of computer time, and by an allocation of Cray YMP time by the San Diego Supercomputer Center.

[1]S. E. Trullinger *et al.*, *Solitons* (North-Holland, Amsterdam, 1986).
[2]R. K. Bullough, Y.-z. Chen, and J. Timonen, in *Nonlinear and Turbulent Processes in Physics,* edited by V. E. Zacharov, A. G. Sitenko, N. S. Erokhin, and V. M. Chernousenko (World Scientific, Singapore, 1990).
[3]E. P. Wigner, Phys. Rev. **40**, 749 (1932).
[4]R. P. Feynman, *Statistical Mechanics* (Benjamin, Reading, MA, 1972).
[5]R. Giachetti and V. Tognetti, Phys. Rev. Lett. **55**, 912 (1985).
[6]R. Giachetti and V. Tognetti, Phys. Rev. B **33**, 7647 (1986).
[7]R. P. Feynman and H. Kleinert, Phys. Rev. A **34**, 5080 (1986).
[8]R. Giachetti, V. Tognetti, and R. Vaia, Phys. Rev. A **37**, 2165 (1988).
[9]R. Giachetti, V. Tognetti, and R. Vaia, Phys. Rev. A **38**, 1521 (1988).
[10]A. Cuccoli, V. Tognetti, and R. Vaia, Phys. Rev. B **41**, 9588 (1990).
[11]S. Liu, G. K. Horton, and E. R. Cowley, Phys. Lett. A **152**, 79 (1990).
[12]A. Cuccoli, A. Macchi, M. Neumann, V. Tognetti, and R. Vaia, Phys. Rev. B **45**, 2088 (1992).
[13]H. Kleinert, Phys. Lett. A **118**, 267 (1986).
[14]R. Vaia and V. Tognetti, Int. J. Mod. Phys. B **4**, 2005 (1990).
[15]A. Cuccoli, V. Tognetti, and R. Vaia, Phys. Rev. A **44**, 2734 (1991).
[16]S. W. Lovesey, *Condensed Matter Physics: Dynamic Correlations* (Benjamin/Cummings, Reading, MA, 1986).
[17]H. Mori, Prog. Theor. Phys. **34**, 399 (1965).
[18]S. W. Lovesey and R. A. Meserve, J. Phys. C **6**, 79 (1972).
[19]K. Tomita and H. Tomita, Prog. Theor. Phys. **45**, 1407 (1971).
[20]H. Tomita and H. Mashiyama, Prog. Theor. Phys. **48**, 1133 (1972).
[21]A. Cuccoli, V. Tognetti, and R. Vaia, Phys. Lett. A **160**, 184 (1991).
[22]F. Gürsey, Proc. Cambridge Philos. Soc. **46**, 182 (1950).
[23]M. Takahashi and M. Imada, J. Phys. Soc. Jpn. **53**, 963 (1984).
[24]M. Takahashi and M. Imada, J. Phys. Soc. Jpn. **53**, 3765 (1984).
[25]See special issue, J. Stat. Phys. **43**, 729 (1986).
[26]R. F. Dashen, B. Hasslacher, and A. Neveu, Phys. Rev. D **10**, 4144 (1974).
[27]K. Maki and H. Takayama, Phys. Rev. B **20**, 3223 (1979).
[28]H. Leschke, in *Path Summation: Achievements and Goals,* edited by S. Lundqvist *et al.* (World Scientific, Singapore, 1988).
[29]H. Janke, in *Path Integrals from meV to MeV,* edited by V. Sa-Yakanit *et al.* (World Scientific, Singapore, 1989).
[30]G. Nienhuis, J. Math. Phys. **11**, 239 (1970).
[31]A. R. Mc Gurn, P. Ryan, A. A. Maradudin, and R. F. Wallis, Phys. Rev. B **40**, 2407 (1989).
[32]D. Thirumalai, E. J. Bruskin, and B. J. Berne, J. Chem. Phys. **79**, 5063 (1983).
[33]D. Thirumalai, R. W. Hall, and B. J. Berne, J. Chem. Phys. **81**, 2523 (1984).
[34]H. Mori, Prog. Theor. Phys. **33**, 423 (1965).
[35]B. J. Berne and R. Pecora, *Dynamic Light Scattering* (Wiley, London, 1976).